for 1 h. After blocking, specimens were incubated with biotin-conjugated anti-B220 mAb for wild-type mice or anti-CD45 mAb for mice on a Rag2$^{-/-}$ background in Solution A containing 0.6% Triton X-100 and 0.1% BSA for 1 h, incubated with ABC reagent (Vector Laboratories) at room temperature for 2 h, and reacted with diaminobenzidene.

We thank Drs. S.-I. Nishikawa and T. W. Mak for valuable materials; Dr. L. K. Clayton for valuable discussion and critical reading of the manuscript; and M. Motouchi and N. Yumoto for animal care. This work was supported by the Waksman Foundation of Japan (S.N.), the Uehara Memorial Foundation, the Tokyo Biochemical Research Foundation, Japan Society for the Promotion of Science Grant-in-Aid 18659141, Scientific Research on Priority Areas Grant-in-Aid 14021110, a National Grant-in-Aid for the Establishment of a High-Tech Research Center in a Private University, a grant for the Promotion of the Advancement of Education and Research in Graduate Schools, and a Scientific Frontier Research Grant from the Ministry of Education, Culture, Sports, Science, and Technology, Japan.

1. Covacci A, Telford JL, Del Giudice G, Parsonnet J, Rappuoli R (1999) *Science* 284:1328–1333.
2. Ernst PB, Gold BD (2000) *Annu Rev Microbiol* 54:615–640.
3. Uemura N, Okamoto S, Yamamoto S, Matsumura N, Yamaguchi S, Yamakido M, Taniyama K, Sasaki N, Schlemper RJ (2001) *N Engl J Med* 345:784–789.
4. Baldari CT, Lanzavecchia A, Telford JL (2005) *Trends Immunol* 26:199–207.
5. Cover TL, Blanke SR (2005) *Nat Rev Microbiol* 3:320–332.
6. Eaton KA, Ringler SR, Danon SJ (1999) *Infect Immun* 67:4594–4602.
7. Pappo J, Torrey D, Castriotta L, Savinainen A, Kabok Z, Ibraghimov A (1999) *Infect Immun* 67:337–341.
8. Panthel K, Faller G, Haas R (2003) *Infect Immun* 71:794–800.
9. Lundgren A, Trollmo C, Edebo A, Svennerholm AM, Lundin BS (2005) *Infect Immun* 73:5612–5619.
10. Yamaguchi H, Osaki T, Takahashi M, Taguchi H, Kamiya S (1999) *FEMS Microbiol Lett* 175:107–111.
11. Reynolds DJ, Penn CW (1994) *Microbiology* 140:2649–2656.
12. Narikawa S, Kawai S, Aoshima H, Kawamata O, Kawaguchi R, Hikiji K, Kato M, Iino S, Mizushima Y (1997) *Clin Diag Lab Immunol* 4:285–290.
13. Bumann D, Habibi H, Kan B, Schmid M, Goosmann C, Brinkmann V, Meyer TF, Jungblut PR (2004) *Infect Immunol* 72:6738–6742.
14. Obonyo M, Guiney DG, Harwood J, Fierer J, Cole SP (2002) *Infect Immun* 70:3295–3299.
15. Frucht DM, Fukao T, Bogdan C, Schindler H, O'Shea JJ, Koyasu S (2001) *Trends Immunol* 22:556–560.
16. Ferlazzo G, Munz C (2004) *J Immunol* 172:1333–1339.
17. Hafsi N, Voland P, Schwendy S, Rad R, Reindl W, Gerhard M, Prinz C (2004) *J Immunol* 173:1249–1257.
18. Lodolce JP, Boone DL, Chai S, Swain RE, Dassopoulos T, Trettin S, Ma A (1998) *Immunity* 9:669–676.
19. Kennedy MK, Glaccum M, Brown SN, Butz EA, Viney JL, Embers M, Matsuki N, Charrier K, Sedger L, Willis CR, *et al.* (2000) *J Exp Med* 191:771–780.
20. Ohteki T, Suzue K, Maki C, Ota T, Koyasu S (2001) *Nat Immunol* 2:1138–1143.
21. Cao X, Shores EW, Hu-Li J, Anver MR, Kelsall BL, Russell SM, Drago J, Noguchi M, Grinberg A, Bloom ET, *et al.* (1995) *Immunity* 2:223–238.
22. Yoshida H, Honda K, Shinkura R, Adachi S, Nishikawa S, Maki K, Ikuta K, Nishikawa SI (1999) *Int Immunol* 11:643–655.
23. Bode G, Mauch F, Malfertheiner P (1993) *Epidemiol Infect* 111:483–490.
24. Dunkley ML, Harris SJ, McCoy RJ, Musicka MJ, Eyers FM, Beagley LG, Lumley PJ, Beagley KW, Clancy RL (1999) *FEMS Immunol Med Microbiol* 24:221–225.
25. Ramarao N, Gray-Owen SD, Backert S, Meyer TF (2000) *Mol Microbiol* 37:1389–1404.
26. Nystrom J, Raghavan S, Svennerholm AM (2006) *Microbes Infect* 8:442–449.
27. Bergman MP, Engering A, Smits HH, van Vliet SJ, van Bodegraven AA, Wirth HP, Kapsenberg ML, Vandenbroucke-Grauls CM, van Kooyk Y, Appelmelk BJ (2004) *J Exp Med* 200:979–990.
28. Emilia G, Longo G, Luppi M, Gandini G, Morselli M, Ferrara L, Amarri S, Cagossi K, Torelli G (2001) *Blood* 97:812–814.
29. Velin D, Bachmann D, Bouzourene H, Michetti P (2005) *Gastroenterology* 29:142–155.
30. Jang MH, Kweon MN, Iwatani K, Yamamoto M, Terahara K, Sasakawa C, Suzuki T, Nochi T, Yokota Y, Rennert PD, *et al.* (2004) *Proc Natl Acad Sci USA* 101:6110–6115.
31. Hamada H, Hiroi T, Nishiyama Y, Takahashi H, Masunaga Y, Hachimura S, Kaminogawa S, Takahashi-Iwanaga H, Iwanaga T, Kiyono H, *et al.* (2002) *J Immunol* 168:57–64.
32. Khin MM, Hua JS, Ng HC, Wadstrom T, Bow H (2000) *World J Gastroenterol* 6:202–209.
33. De Vita S, Ferraccioli G, Avellini C, Sorrentino D, Dolcetti R, Di Loreto C, Bartoli E, Boiocchi M, Beltrami CA (1996) *Gastroenterology* 110:1969–1974.
34. Kroneld U, Jonsson R, Carlsten H, Bremell T, Johannessen AC, Tarkowski A (1998) *Scand J Rheumatol* 27:215–218.
35. Suzuki H, Duncan GS, Takimoto H, Mak TW (1997) *J Exp Med* 185:499–505.
36. Leder LD (1979) *Am J Dermatopathol* 1:39–42.
37. Lorenz RG, Chaplin DD, McDonald KG, McDonough JS, Newberry RD (2003) *J Immunol* 170:5475–5482.

Sphingosine 1-phosphate dependence in the regulation of lymphocyte trafficking to the gut epithelium

Jun Kunisawa,[1,2] Yosuke Kurashima,[1,2] Morio Higuchi,[1,2] Masashi Gohda,[1,2] Izumi Ishikawa,[1,2] Ikuko Ogahara,[1,2] Namju Kim,[1,2] Miki Shimizu,[1,2] and Hiroshi Kiyono[1,2]

[1]Division of Mucosal Immunology, Department of Microbiology and Immunology, The Institute of Medical Science, University of Tokyo, Minato-ku, Tokyo 108-8639, Japan
[2]Core Research for Evolutional Science and Technology, Japan Science and Technology Corporation, Kawaguchi, Saitama 322-0012, Japan

It is well established that intraepithelial T lymphocytes (IELs) are derived from conventional single-positive (SP) thymocytes, as well as unconventional double-negative (DN) thymocytes and CD103$^+$CD8αβ recent thymic emigrants (RTEs). We show that IELs can be divided into two groups according to their dependency on sphingosine 1-phosphate (S1P) for trafficking into the intestines. CD4 or CD8αβ naive lymphocytes originating from SP thymocytes express high levels of type 1 S1P receptor ($S1P_1$), and their preferential migration into the large intestine is regulated by S1P. In contrast, RTEs migrate exclusively into the small intestine, whereas DN thymic IEL precursors expressing either TCRαβ or TCRγδ migrate into both the small and large intestines. S1P does not play a role in the migration pathways of these unconventional thymic IEL precursors. Thus, down-regulation of $S1P_1$ expression or disruption of the S1P gradient halted conventional CD4 or CD8αβ IEL trafficking into the intestines, but did not affect the trafficking of unconventional thymic IEL precursors. These data are the first to demonstrate that a lipid-mediated system discriminates IELs originating from conventional and unconventional thymic precursors.

CORRESPONDENCE
Hiroshi Kiyono:
kiyono@ims.u-tokyo.ac.jp

Abbreviations used: CCR9, CC chemokine receptor 9; CP, colonic patch; DN, double-negative; DOP, deoxypyridoxine; DP, double-positive; EC, epithelial cell; IEL, intraepithelial T lymphocyte; IBD, inflammatory bowel disease; MLN, mesenteric LN; PP, Peyer's patch; RTE, recent thymic emigrant; S1P, sphingosine 1-phosphate; $S1P_1$, type 1 S1P receptor; SLN, sacral LN; SP, single-positive; z TN, triple-negative; TP, triple-positive.

The gastrointestinal tract harbors numerous luminal foreign antigens, including food products and commensal and pathogenic microorganisms. To maintain appropriate homeostasis in this harsh environment, both innate and acquired immunity are required (1–3). In the intestinal epithelium, innate and acquired mucosal immunity are bridged in part by intraepithelial T lymphocytes (IELs) located between epithelial cells (ECs) (4, 5). Previous studies of small intestinal IELs have shown them to possess several features that distinguish them from peripheral T cells. For instance, small intestinal IELs are composed of conventional CD4 and CD8αβ cells, as well as unique cells expressing CD8α as a homodimer (CD8αα) with either TCRαβ or TCRγδ (4, 5). Additionally, in contrast to the strict selection of CD4 and CD8αβ T cells in the thymus, CD8αα IELs possess several unique developmental pathways (6–12).

Several lines of evidence have demonstrated that the composition of IELs in the large intestine differs from that in the small intestine (4, 13–15), but the molecular mechanism underlying this distinction has remained obscure. Its identification would greatly improve our understanding of immune surveillance and homeostasis in the intestine, as the physiological function and surrounding microenvironment of these two portions of the digestive tract are different.

Recently, sphingosine 1-phosphate (S1P) has received considerable attention for its biological activity against different cell types, including lymphocytes (16, 17). To date, five S1P receptors have been identified, each of which associates with a different type of G protein, resulting in a distinct signal transduction (16, 17). Mounting evidence demonstrates that lymphocytes preferentially express type 1 S1P receptor ($S1P_1$) and $S1P_4$, and the former has been shown to regulate lymphocyte emigration from the thymus and secondary lymphoid organs (18, 19).

The online version of this article contains supplemental material.

JEM © The Rockefeller University Press $30.00
Vol. 204, No. 10, October 1, 2007 2335-2348 www.jem.org/cgi/doi/10.1084/jem.20062446

Supplemental Material can be found at:
http://www.jem.org/cgi/content/full/jem.20062446/DC1

FTY720 binds to four types of S1P receptor, including $S1P_1$, and induces down-regulation of their expression on thymocytes and lymphocytes (18, 20, 21). Thus, FTY720 induces lymphocyte sequestration in lymph and blood by inhibiting lymphocyte emigration from the secondary lymphoid organs and thymus (18, 20–22). In addition, a recent study demonstrated that oral administration of deoxypyridoxine (DOP), which is a vitamin B6 antagonist, increases S1P concentration in the thymus and secondary lymphoid organs by inhibiting S1P degradation (23). This increased S1P concentration causes lymphocytes to accumulate in the thymus and simultaneously to be depleted from the blood and lymph (23). We recently revealed that S1P also plays an important role in the regulation of peritoneal B cell trafficking into intestinal compartments for intestinal secretory IgA production (24). Although these findings suggest that S1P plays an essential role in the regulation of lymphocyte trafficking in both systemic and mucosal immunity, its involvement in IEL trafficking remains largely unknown.

In this study, we aimed to elucidate the role of S1P in the trafficking of the different subsets of small and large intestinal IELs. We present evidence that the proportion of $S1P_1^+$ and $S1P_1^-$ IELs differs in the small and large intestines. We also show that S1P regulates the migration of $S1P_1^+$ naive IELs into the intestinal compartments through secondary lymphoid organs. In addition, we demonstrate that recent thymic emigrants (RTEs) preferentially migrate into the small intestine, whereas double-negative (DN) thymocytes expressing either TCRαβ or TCRγδ migrate into both the small and large intestines. Thus, IEL trafficking from the thymus into the intestines was not regulated by S1P-mediated pathways.

RESULTS

FTY720 reduces CD8αβ and CD4 IELs in the large intestine and some populations of CD4 IELs in the small intestine

We initially tested whether IEL populations in the small and large intestines were affected by treatment with FTY720. Confirming the findings of a previous study (25), we showed that 5 d of treatment with FTY720 reduced the total cell numbers in the spleen without affecting the cell composition (Fig. S1 A, available at http://www.jem.org/cgi/content/full/jem.20062446/DC1). We also observed increased numbers of single-positive (SP) thymocytes, whereas $CD8^+$ or $CD4^+$ cells were markedly reduced in the liver of mice receiving FTY720 (Fig. S1 A) (22). In these mice, a significant reduction in IEL numbers was observed in the large intestine, with a more modest reduction noted in small intestine (Fig. 1 A). Based on these findings, we focused our initial experiment on large intestinal IELs. Flow cytometric analysis revealed that FTY720 treatment almost completely suppressed CD4 IELs, which are a major population of large intestinal IELs, but increased the number of CD8α cells in the $CD3^+$ T cell fraction (Fig. 1 B). Of the two subsets found in the large intestine CD8α IEL fraction, the CD8αβ IELs were dramatically decreased by FTY720 treatment, whereas the CD8αα IELs showed an increase (Fig. 1 B). Calculation of the absolute cell numbers indicated a marked decrease in cell numbers of CD4 IELs and CD8αβ IELs, but a slight increase in CD8αα IELs after FTY720 treatment (Fig. 1 C).

We next used quantitative RT-PCR to test whether the sensitivity of large intestinal IELs to FTY720 was attributable to the expression of S1P receptors. We found that FTY720-sensitive CD4 IELs and CD8αβ IELs expressed high levels of $S1P_1$, whereas FTY720-insensitive CD8αα IELs showed barely detectable levels of $S1P_1$ (Fig. 1 D). Despite their high expression of $S1P_1$, large intestinal CD4 IELs and CD8αβ IELs showed lower, and sometimes barely detectable, levels of other types of S1P receptor ($S1P_3$ and $S1P_4$; unpublished data).

We next sought to determine whether FTY720 treatment had to be continuous to block S1P-mediated signals, leading to decreased numbers of large intestinal CD4 and CD8αβ IELs. In this experiment, mice were injected with FTY720 once daily for several days, and the large intestinal IEL population was examined 12 h after each injection. Dramatic reductions in CD4 and CD8αβ IEL numbers were observed after a single injection of FTY720, but additional injections did not enhance this effect (Fig. 1 E). We next analyzed the kinetics of IEL recovery after a single FTY720 treatment. A partial recuperation was detected on day 3, with full recovery observed 7 d after the injection (Fig. 1 F). These data suggest that the effect of FTY720 on large intestinal CD4 IELs and CD8αβ IELs is rapid, but reversible.

As it is well established that intestinal IELs, especially CD8αα IELs, uniquely express either TCRαβ or TCRγδ (4, 5), we set out to determine whether FTY720 treatment influenced the pattern of TCR expression by various subsets of large intestinal IELs. We found that CD8αβ IELs and CD4 IELs in the large intestine expressed TCRαβ, but not TCRγδ, and that both populations of IELs were significantly reduced when mice received FTY720 (Fig. 1 G). In contrast,

Figure 1. FTY720 treatment dramatically reduces CD4 IEL and CD8αβ IEL numbers in the large intestine, and modestly reduces CD4 IELs in the small intestine. (A) BALB/c mice received 1 mg/kg FTY720 (shaded bar) or water (open bar) for 5 d. IELs were collected from large (left) and small (right) intestines 12 h after the final administration of FTY720. The data represent the mean ± the SEM of eight independent experiments. (B) Flow cytometric analysis was performed to determine the cell population in the $CD3^+$ fraction of the large intestinal IELs affected by FTY720. The data are representative of five independent experiments. (C) Cell numbers of each population were calculated using the total cell number and flow cytometric data. The error bars represent the average ± the SEM ($n = 5$). (D) Quantitative RT-PCR analysis for $S1P_1$ was performed using RNA isolated from the sorted large intestinal IELs and splenocytes. The relative mRNA was expressed as a ratio to GAPDH. (E) BALB/c mice received a daily intraperitoneal injection of FTY720. At 12 h after each injection, the large intestinal IELs were analyzed by flow cytometry (square, CD4; triangle, CD8αβ; circle, CD8αα). The data represent the means ± the SD ($n = 5$). (F) Flow cytometry was used to evaluate the degree of IEL recovery in the large intestine after one administration of FTY720 (square, CD4; triangle, CD8αβ; circle, CD8αα). The data represent the means ± the SD ($n = 5$). (G) TCRαβ versus TCRγδ expression on large intestinal IELs of

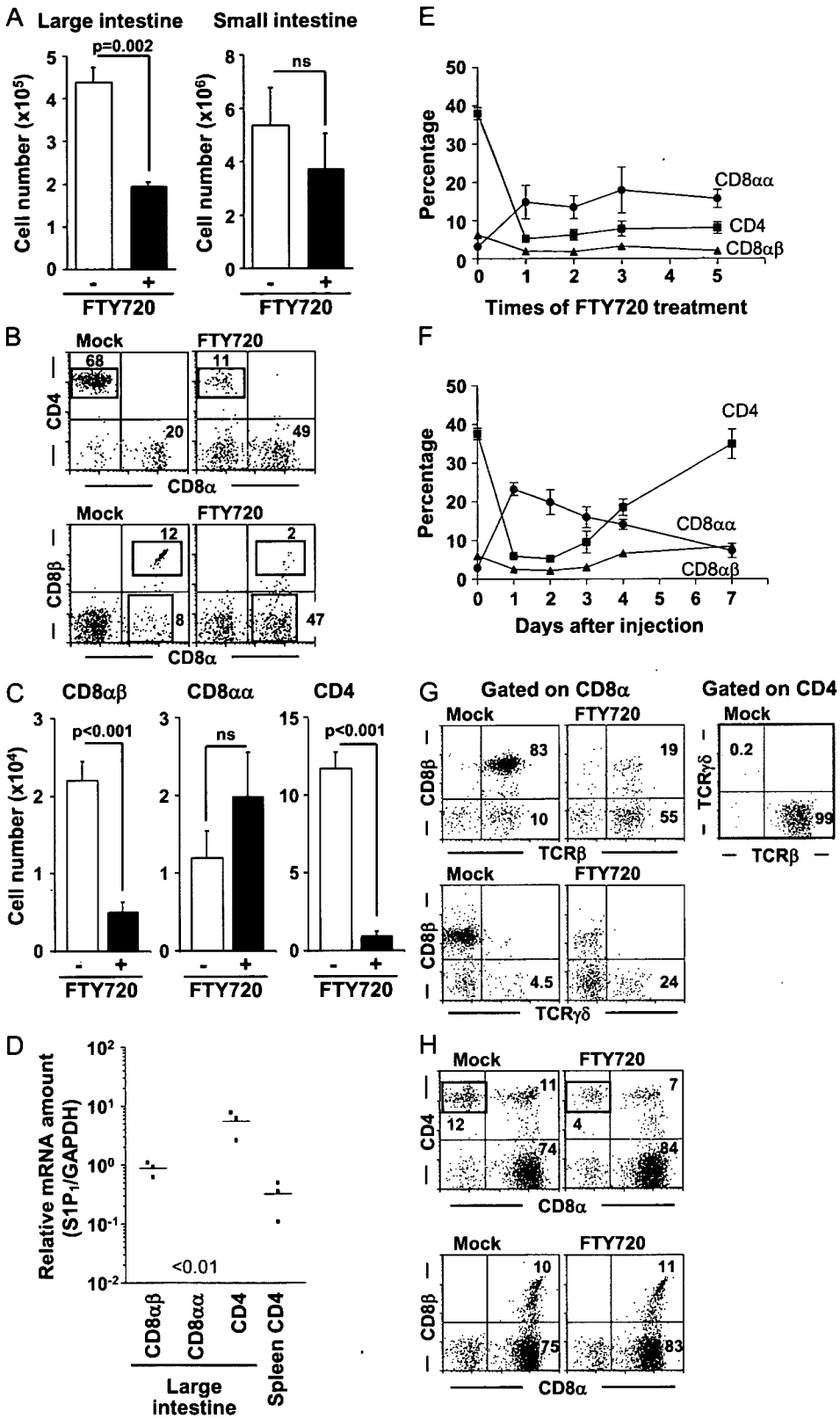

mice receiving 5 doses of 1 mg/kg FTY720 or water (mock). The data for cells gated on CD8α (left) and CD4 (right). The data are representative of four independent experiments. (H) Flow cytometric analysis was performed to identify the cell population in $CD3^+$ cells in small intestinal IELs affected by FTY720. The data are representative of five independent experiments.

65% of CD8αα IELs expressed TCRαβ, whereas the remaining 35% expressed T CRγδ. The ratio between TCRαβ (68%) and TCRγδ (32%) in the CD8αα IELs was not changed by FTY720 treatment (Fig. 1 G), although a modest increase in the number of CD8αα IELs was observed (Fig. 1 C). These data suggest that the efficacy of FTY720 treatment does not depend on TCR expression.

As FTY720 induced a reduction in small intestinal IEL numbers, albeit a more modest one than in the large intestine (Fig. 1 A), we next focused on the small intestinal IELs. Flow cytometric analysis indicated that CD4 IELs were significantly decreased by FTY720 treatment (mock, 13.7 ± 0.89% vs. FTY720, 5.7 ± 1.21%; P = 0.006), whereas CD4CD8 double-positive (DP) IEL numbers were unaltered and CD8α-positive cells were increased in $CD3^+$ fractions (Fig. 1 H). We found a modest enhancement of CD8αα IELs, but only a slight increase in CD8αβ IELs (Fig. 1 H). Although FTY720 was observed to affect intestinal IELs, it had no influence over Peyer's patches (PPs) in the small intestine or colonic patches (CPs) and small lymphoid aggregates in the large intestine (Fig. S1, A and B). We also confirmed that the epithelium was specifically removed during the separation process of IELs (Fig. S1 C), and found that similar results were obtained when saline perfusion was performed before tissue isolation (unpublished data). These findings suggest that the reduction of CD4 and CD8αβ lymphocytes occurred specifically in the IEL population, and was not caused by contamination from other tissues.

The specific expression pattern of adhesion molecules correlates with the sensitivity of small and large intestinal IELs to FTY720

Tissue-specific lymphocyte trafficking is regulated by a combination of adhesion molecules and chemokines. In the current study, we focused on two representative adhesion molecules expressed specifically on gut-associated lymphocytes: α4β7 integrin and CD103 (αE integrin) (26, 27). Each population of small and large intestinal CD4 IELs has its own distinct expression pattern (Fig. 2). All CD4 IELs express α4β7 integrin, but ~80% of CD4 IELs in the small intestine are $CD103^-$ (Fig. 2 A). After FTY720 treatment, the small intestinal epithelia of mice showed a simultaneous decrease in the percentage of $CD103^-$ CD4 IELs and an increase in the percentage of $CD103^+$ cells (Fig. 2 A). Because CD4 IELs include CD4 SP cells and CD4CD8 DP cells (Fig. 1 H), we determined that the $CD103^-CD4^+$ population contained a larger number of CD4 SP cells than DP cells, whereas DP cells comprised the majority of the $CD103^+$ CD4 cell population (Fig. 2 A). FTY720 treatment preferentially reduced CD4 SP cells, but had little effect on DP cells, suggesting that $CD103^-$ CD4 SP cells were the main target cell of FTY720 in the small intestine (Fig. 2 A). We further divided small intestinal CD4 IELs according to their expression of CD62L, finding that $CD103^+$ CD4 IELs do not express CD62L, whereas $CD103^-$ CD4 IELs comprise three populations expressing different levels of CD62L ($CD62L^{high}$, $CD62L^{int}$, and $CD62L^{neg}$; Fig. 2 A). Of these three populations, only $CD62L^{high}CD103^-$ CD4 IELs were completely vanished from the small intestinal epithelium after FTY720 treatment (Fig. 2 A).

Although the various subsets of small intestinal CD4 IELs express variable levels of CD103, consistently high levels of CD103 are expressed by both CD8αα IELs and CD8αβ IELs (Fig. 2 A). Nonetheless, a few CD8αβ IELs did not express CD103, but exhibited high levels of CD62L (Fig. 2 A). As with $CD62L^{high}CD103^-$ CD4 IELs (Fig. 2 A), the $CD62L^{high}CD103^-$ CD8αβ IELs were effectively suppressed by FTY720 treatment (Fig. 2 A). Quantitative RT-PCR analysis demonstrated that the level of $S1P_1$ expression in $CD62L^{high}$ cells was greatly higher than in $CD62L^{neg}$ cells (Fig. 2 B), suggesting that the expression pattern of CD62L and CD103 in the small intestinal IELs correlates with the sensitivity to FTY720. Collectively, these findings show that S1P is primarily responsible for regulating the trafficking of $CD62L^{high}CD103^-$ IELs expressing either CD4 or CD8αβ in the small intestinal epithelium.

In the next series of experiments, we sought to characterize the association between the expression of these adhesion molecules and FTY720 sensitivity in large intestinal IELs. FTY720-sensitive large intestinal CD4 IELs and CD8αβ IELs expressed the α4β7 integrin and high levels of CD62L, with negative or intermediate levels of CD103 ($CD103^{int/neg}$; Fig. 2 C), which is similar to the FTY720-sensitive $CD62L^{high}$ $CD103^-$ population in the small intestinal IELs (Fig. 2 A). In contrast, the FTY720-insensitive CD8αα population expressed high levels of CD103, but did not express the α4β7 integrin and CD62L (Fig. 2 C). Confocal microscopic analysis confirmed the presence of $CD62L^+$ CD4 cells in the large intestinal epithelium and FTY720 treatment removed them, providing convincing evidence of a correlation between $CD62L^{high}CD103^{int/neg}$ cells and the sensitivity of small and large intestinal IELs to FTY720 (Fig. 2 D). Because sacral LNs (SLNs) act as draining LNs for the large intestine, we next set out to examine FTY720-induced alterations in SLN cell populations, demonstrating that FTY720 increased the number of $CD62L^{high}$ cells in the SLN (Fig. 2 E).

Lymphocyte migration is regulated not only by integrins, but also by chemokines. S1P is thought to be a modulator of cellular responses to some chemokines (17), and CC chemokine receptor 9 (CCR9) is believed to be involved in the migration of lymphocytes into the intestinal compartment, especially the small intestine (28). Thus, we next investigated whether distinct CCR9 expression patterns were observed for FTY720-sensitive and -insensitive IELs. We found that CD8αβ and CD8αα IELs in the small and large intestines expressed varying levels of CCR9 (Fig. S2, available at http://www.jem.org/cgi/content/full/jem.20062446/DC1). The CD8αβ population in the large intestinal epithelium was reduced after FTY70 treatment, regardless of CCR9 expression (Fig. S2). Additionally, no change in the ratio of $CCR9^+$ and $CCR9^-$ populations in CD8αα IELs was observed after FTY720 treatment (Fig. S2). Hence, the CCR9 expression level does not seem to be linked to the S1P-mediated migration of small and large intestinal IELs.

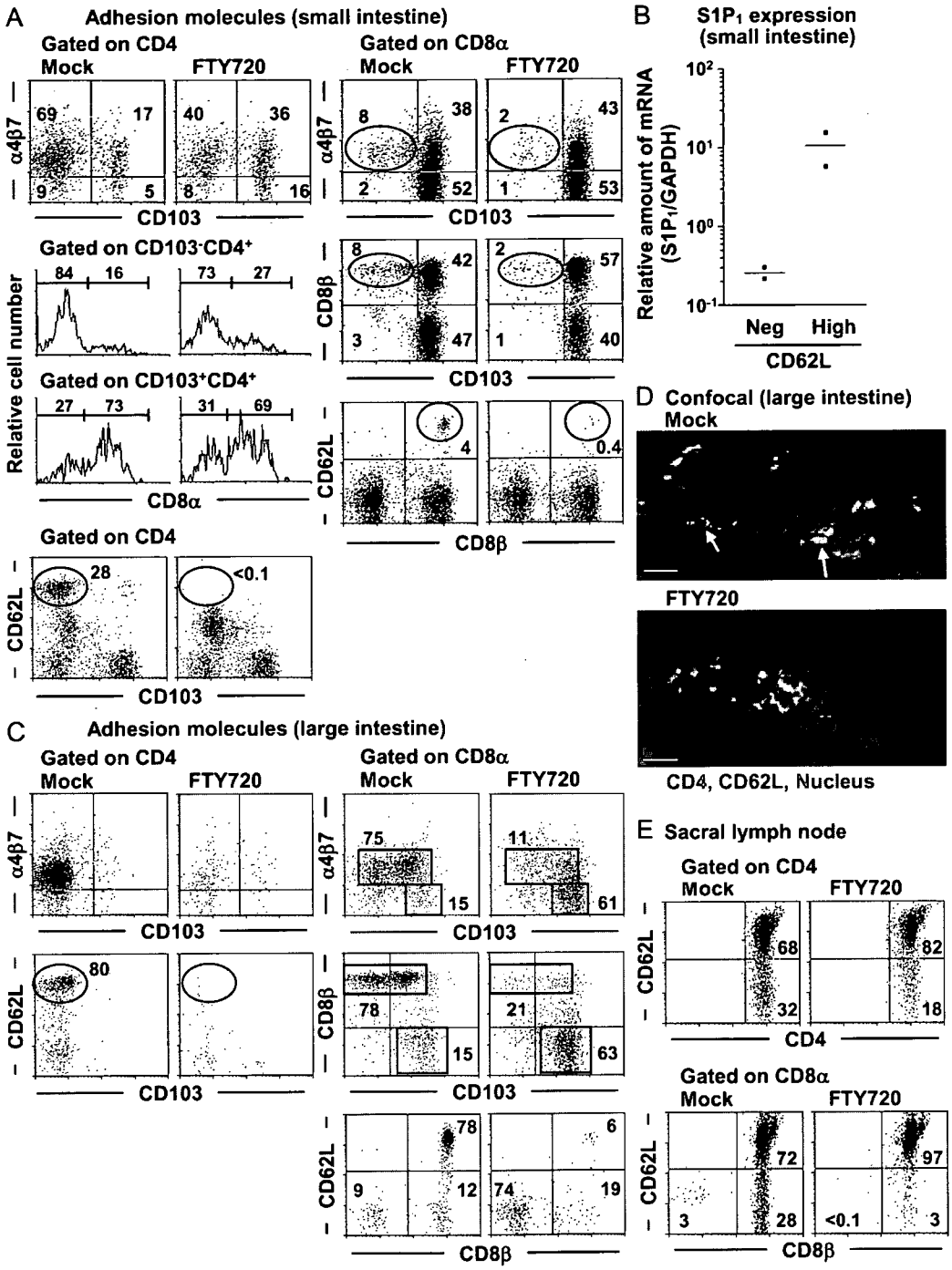

Figure 2. Unique expression of adhesion molecules determines the sensitivity of small and large intestinal IELs to FTY720. (A) Small intestines of BALB/c mice that were treated with FTY720 or water (mock) isolated for flow cytometric analysis of the adhesion molecule expression patterns. Flow cytometric profiles of cells gated on CD4 (left), $CD103^{-}CD4^{+}$ (left), $CD103^{+}CD4^{-}$ (left), and CD8α (right) were shown. The data are representative of five independent experiments. (B) Quantitative RT-PCR analysis for $S1P_1$ on RNA isolated from sorted small intestinal CD4 IELs expressing $CD62L^{high}$ or $CD62L^{-}$. The relative mRNA is expressed as a ratio to GAPDH. (C) Experiments similar to those shown in A were performed using large intestinal IELs. Similar results were obtained from five independent experiments. (D) Confocal microscopic analysis of the large intestine was performed using antibodies for CD4 (green) and CD62L (red), and DAPI (blue) for counterstaining. Bars, 20 μm. (E) Lymphocytes were isolated from SLN after five doses of FTY720 as shown in A and C, and were examined for the indicated populations by flow cytometry. Experiments were repeated three times.

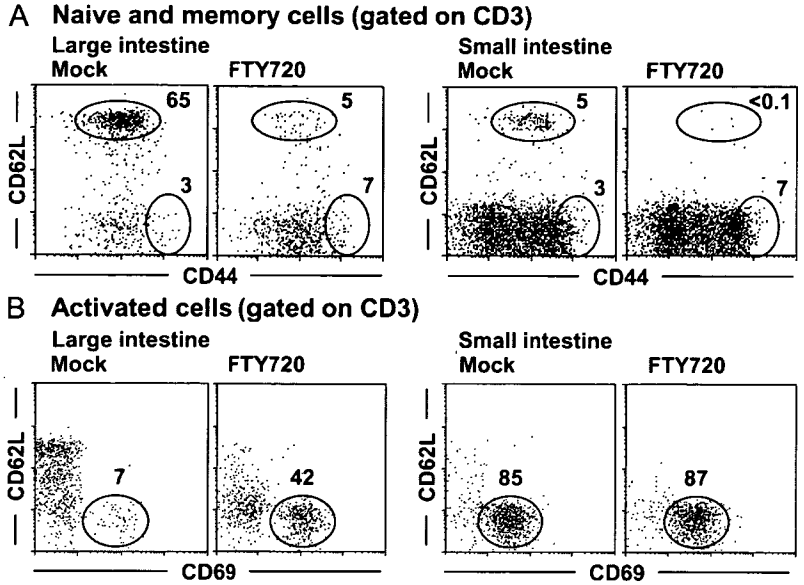

Figure 3. FTY720 selectively suppresses naive-type IELs in both the small and large intestines. IELs were isolated from the small and large intestines of mice receiving FTY720, as shown in Fig. 1. Flow cytometry was used to analyze the effects of FTY720 on naive ($CD62L^{high}CD44^{int}$; A) and activated ($CD62L^{neg}CD69^{+}$; B) IELs in the $CD3^{+}$ population. The data are representative of four independent experiments.

Naive IELs are the main targets of FTY720 in the intestinal epithelium

The high levels of CD62L expression by FTY720-sensitive cell populations (Fig. 2) led us to hypothesize that FTY720 influences naive IELs. To test this, we examined CD44, CD69, and CD62L expression patterns to determine their qualification for naive and activated cells (Fig. 3). We found that large intestinal epithelia contained greater numbers of naive cells expressing $CD62L^{high}CD44^{int}$ than did small intestinal epithelia; however, despite this difference, naive IELs in both the small and large intestines were almost completely suppressed after FTY720 treatment (Fig. 3 A). In contrast, mice receiving FTY720 showed comparable numbers of $CD62L^{neg}CD69^{+}$-activated IELs in the small intestine and an increased percentage in the large intestine (Fig. 3 B). Although FTY720 significantly affected naive IELs, it had almost no influence on naive cells in the PPs (Fig. S3, available at http://www.jem.org/cgi/content/full/jem.20062446/DC1A). These findings suggest that the trafficking of naive IELs is solely regulated by S1P in the small and large intestines, and that the differing sensitivities of the small and large intestines to FTY720 can be attributed to differences in the composition of these naive cells.

FTY720 affects IEL migration and retention, but not cell activation

To determine whether FTY720 reduced naive IELs by inhibiting cell migration into the intestine, we intravenously transferred CFSE-labeled T cells isolated from mesenteric LNs (MLNs) and SLNs into mice and examined their migration into the intestinal compartments. As previously documented (18, 20–22), the number of $CFSE^{+}$ T cells decreased in the blood of mice treated with FTY720 both 1 and 7 d after the transfer (Fig. 4 A). In these mice, migration of $CFSE^{+}$ cells into the MLN and SLN was reduced by FTY720 treatment, whereas that into the PPs was increased (Fig. 4, B–D), which was consistent with a previous study (29). Flow cytometric analysis of $CFSE^{+}$ cells in these tissues revealed that their naive cell phenotype persisted after FTY720 treatment (Fig. 4, B–D). We also found $CFSE^{+}$ cells in the large intestinal epithelium 1 d after the transfer, but the numbers of these cells were significantly decreased in mice treated with FTY720 (Fig. 4 E). Consistent with a previous work (30), fewer cells migrated into the small intestine than the large intestine under these experimental conditions (<0.01% cells were $CFSE^{+}$ 1 d after the transfer; unpublished data). However, similar results were obtained in both the small and large intestines 7 d after transfer, demonstrating that the migration of $CFSE^{+}$ cells was significantly curtailed by FTY720 in both the small and large intestines (Fig. 4 E). We obtained similar results when T cells isolated from GFP-transgenic mice were used instead of the CFSE-labeled system, ruling out the possibility that the $CFSE^{+}$ cell numbers in FTY720-treated mice were reduced because of cell division during these 7 d (unpublished data). These findings suggest that prevention of ongoing naive cell homing into the gut from the systemic immune compartments is one mechanism of FTY720-induced naive IEL reduction.

As shown in Fig. 1 H, FTY720-mediated reduction of naive IELs was rapid (within 12 h). If this is attributable only to the inhibition of naive cell entry into the intestine, the turnover rate in the intestinal epithelium should be <12 h. To examine this, we performed a BrdU time course study of IELs.

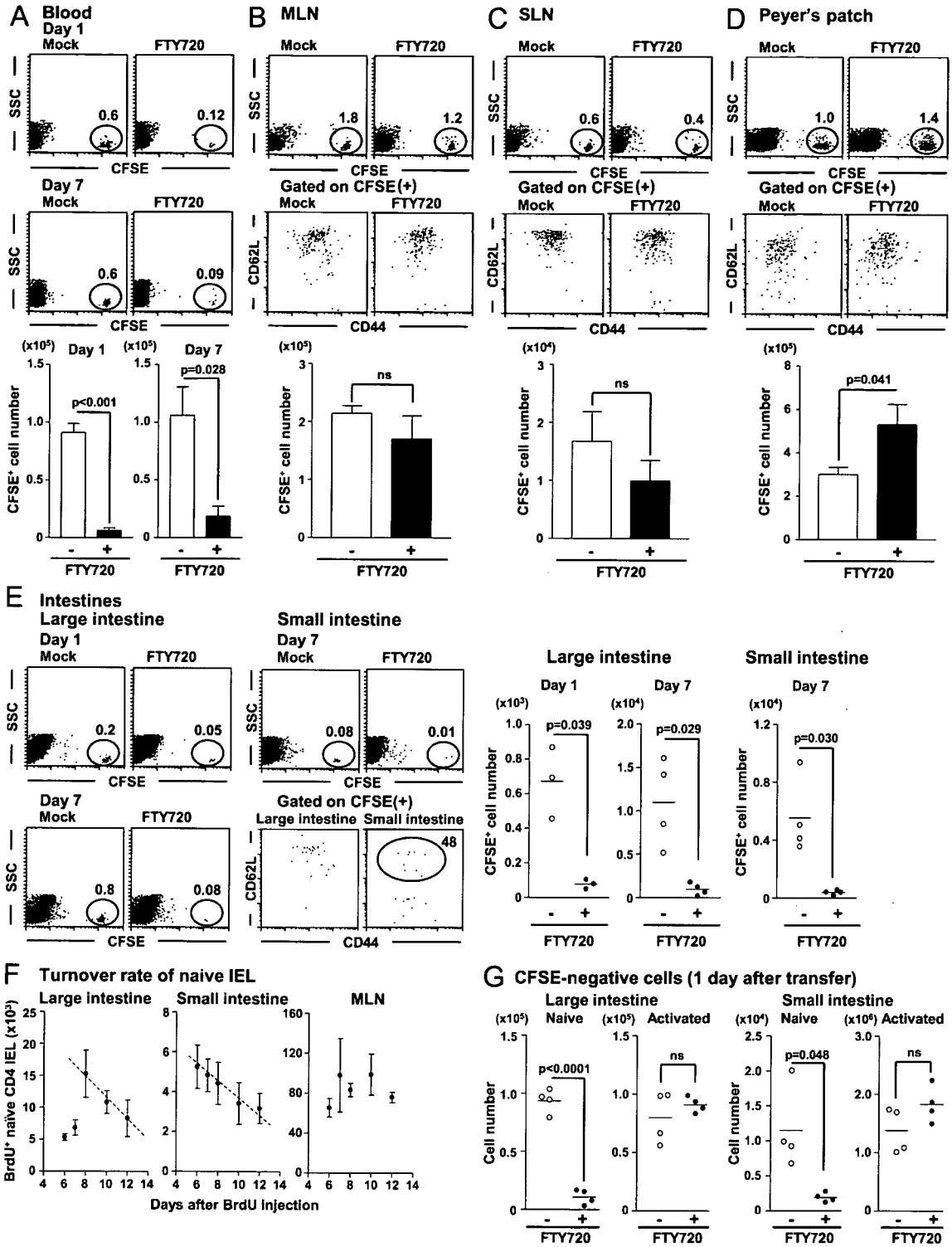

Figure 4. FTY720 inhibits T cell migration to the intestine and retention in the intestinal epithelium without affecting cell activation. (A–E) On day 1 (blood and large intestine) or day 7 (all tissues) after the adoptive transfer of CFSE-labeled T cells, cells were isolated from the blood (A), MLN (B), SLN (C), PP (D), and intestinal epithelium (E) of mice treated with water (mock, open) or FTY720 (filled), and the total number of $CFSE^+$ cells was examined. The data are representative of four independent experiments, and graph data represent means ± SEM ($n = 4$). (F) Cell numbers of $BrdU^+$ naive ($CD62L^{high}$) CD4 IELs measured in large (left) and small (center) intestinal epithelia and MLN (right) of mice from day 6 to 12 after a single BrdU injection. The data represent the means ± the SEM ($n = 5$). (G) Cell numbers of naive ($CD62L^{high}$ and $CD44^{int}$) and activated ($CD62L^-$ and $CD69^+$) cells in $CFSE^-$ populations were measured in the small and large intestinal epithelia of mice receiving mock (open circle) or FTY720 (filled circle) treatment (right) 24 h after transfer.

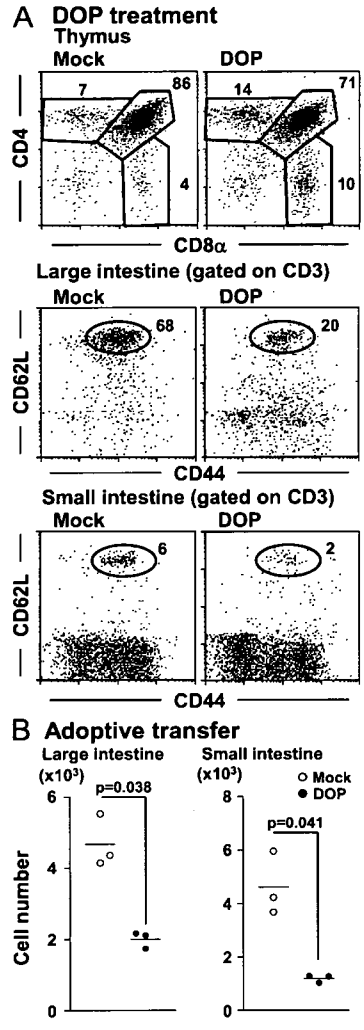

Figure 5. Disruption of S1P gradient halts naive IEL migration. (A) Lymphocytes were collected from the thymus (top) and large (middle) and small (bottom) intestines of mice treated with DOP (right) or water (left) for 3 d, and were analyzed for naive cells in the $CD3^+$ population. The data are representative of three independent experiments. (B) At 7 d after the adoptive transfer of CFSE-labeled T cells, cells were isolated from the large (left) or small (right) intestinal epithelia of mice treated with mock (open circle) or DOP (filled circle), and the total number of $CFSE^+$ cells was examined.

By 6 d after the single BrdU injection, BrdU-labeled cells were barely detected in the thymus (unpublished data), indicating that newly developed naive T cells were BrdU negative. The number of $BrdU^+$ naive CD4 IELs started to fall on day 8 in the large intestine and day 6 in the small intestine, after a linear regression (Fig. 4 F). The estimated 50% turnover rates of naive CD4 IELs were >3 d in both small and large intestines (Fig. 4 F). In contrast, the cell number of $BrdU^+$ cells in the MLN was maintained at a similar level during the experiment, excluding the possibility that the decay curves reflected the survival time of $BrdU^+$ cells. These findings led us to suggest that FTY720 affects naive IEL retention in the intestinal epithelium, which would lead to a reduction in the number of $CFSE^-$ IELs. To test this hypothesis, we examined $CFSE^-$ cells in the intestines 1 d after the transfer because few cells migrated into the intestinal epithelium after this time under this experimental condition (Fig. 4 E). We observed a significant decrease in naive ($CD62L^{high}CD44^{int}$), but not in activated ($CD62L^{neg}CD69^+$), CFSE-negative cells residing in the small and large intestines of FTY720-treated mice (Fig. 4 G). To examine the possibility that FTY720 treatment could lead to the disappearance of resident naive IELs by triggering either the activation of naive IELs or their programmed cell death, we next cultured naive lymphocytes with FTY720 for 2 d and examined their phenotype and viability and noted no changes in either cell activation or viability (Fig. S3 B and not depicted). These findings suggest that FTY720 inhibits not only naive lymphocyte migration into the intestine from the systemic immune compartments but also their retention in the intestinal epithelium.

Inhibiting S1P lyase activity disrupts the S1P gradient and hampers cell trafficking into the intestine

To further confirm the involvement of S1P in the regulation of IEL trafficking, we next used DOP, which was reported to disrupt the S1P gradient by inhibiting S1P lyase (23). Our results confirmed this, and demonstrated that disruption of the S1P gradient by oral feeding with DOP for 3 d resulted in the accumulation of SP thymocytes (Fig. 5 A). DOP treatment also reduced the number of naive IELs in both the small and large intestines (Fig. 5 A). An adoptive-transfer experiment using CFSE-labeled naive T cells revealed that DOP treatment inhibited their trafficking into the intestines (Fig. 5 B). These findings convincingly demonstrated that an S1P-mediated pathway regulates the naive IEL trafficking.

FTY720-insensitive trafficking of unconventional thymic IEL precursors into the intestinal epithelium

Our focus was next shifted to FTY720-insensitive IEL populations, such as CD8αα IELs. Recent studies have revealed several distinctive developmental pathways for IELs, including unconventional thymic IEL precursors (6–11). Thus, we examined whether S1P mediated the migration of these thymus-originated IEL precursors into the small and large intestines using the intrathymic FITC-labeling system. By 24 h

Figure 6. FTY720-insensitive migration of RTEs and thymic DN IEL precursors expressing TCRαβ or TCRγδ into the intestinal epithelium. By 24 h after intrathymic FITC injection, the cell populations in $FITC^+$ and $FITC^-$ thymocytes (A) in mock-treated (left) or FTY720-treated (right) mice were examined by flow cytometry. Cells were isolated from the blood (B), MLN (C), large intestine (D), and small intestine (E) and examined by flow cytometry. Absolute cell numbers of $FITC^+$ cells were calculated using the total cell numbers and flow cytometric data. Expression of CD4, CD8α, CD8β, CD11b, CD11c, CD103, c-kit, IL-7R, TCRαβ, and TCRγδ was examined in $FITC^+$ cells. The graph data depicts the means ± the SEM ($n = 4$). Other data are representative of at least four independent experiments.

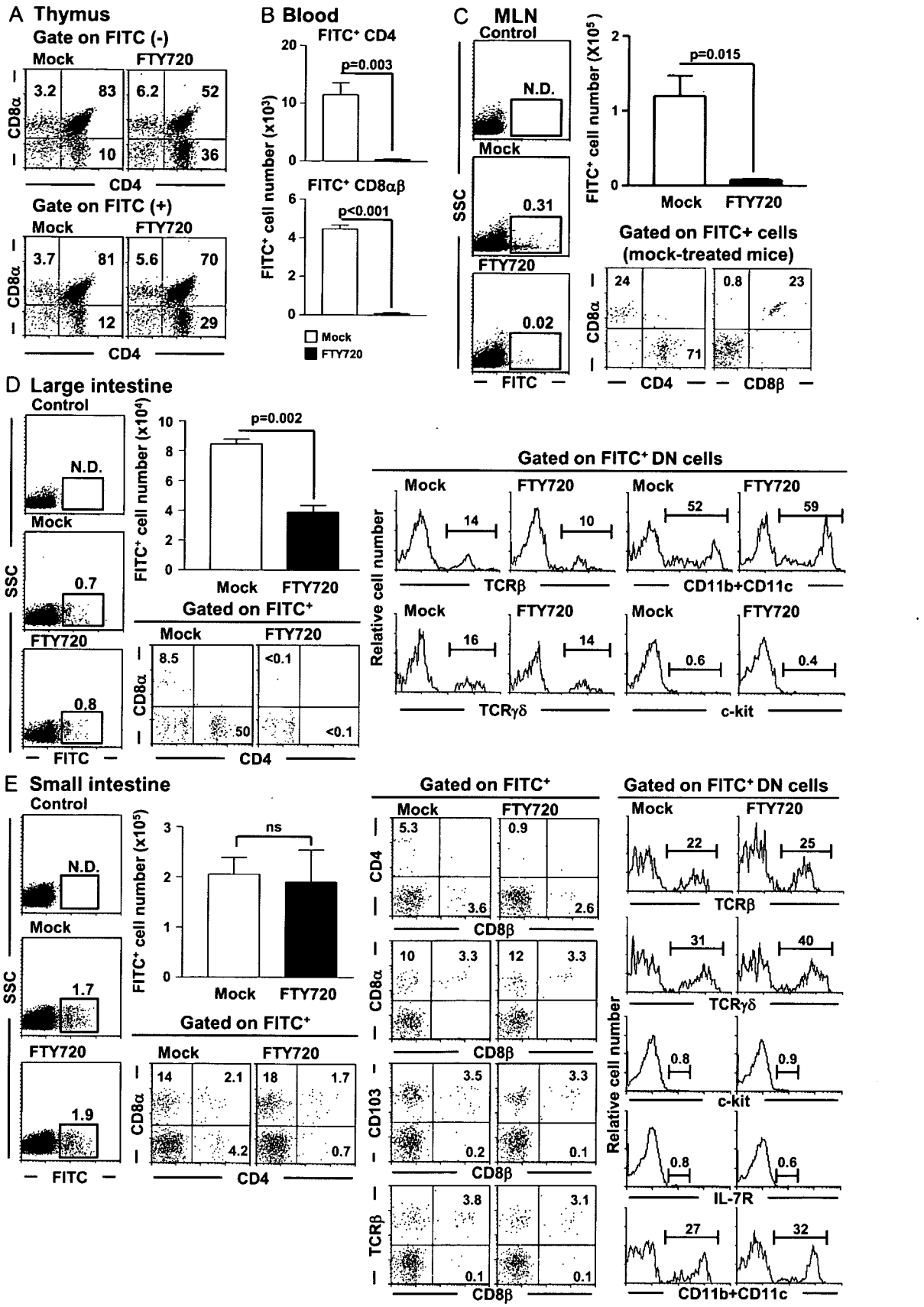

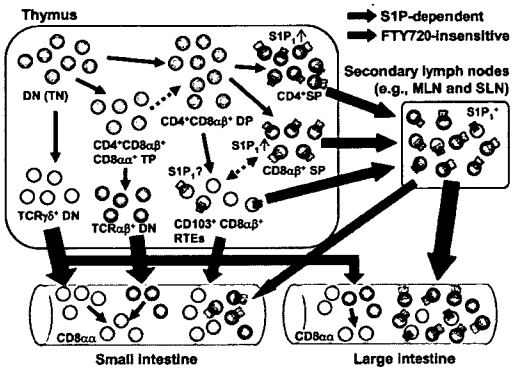

Figure 7. Dependency of lymphocyte migration into the small and large intestines on S1P. Conventional CD4 (green) and CD8 (orange) SP thymocytes emigrate from the thymus into secondary lymphoid organs, and, subsequently, into the small and large intestines. These SP cells express high levels of $S1P_1$ and pathways regulated by S1P (blue lines), and can be inhibited by FTY720. Unconventional thymic IEL precursors, including mature post-selected TCRαβ DN cells (red) derived from TP ($CD4^-CD8\alpha\beta^+CD8\alpha\alpha^+$) thymocytes (pink), TCRγδ DN thymocytes (purple), and $CD103^+$ CD8αβ RTEs (yellow), migrate into the intestinal epithelium through FTY720-insensitive pathways (red lines).

after the intrathymic FITC injection, we found that each population of thymocytes was equally stained with FITC. Thus, comparable percentages of CD4 and CD8 SP, DP, and DN thymocytes were found in $FITC^+$ and $FITC^-$ thymocytes in mock-treated control mice (Fig. 6 A). Additionally, FTY720 treatment resulted in similar accumulation levels of CD4 and CD8 SP thymocytes in both $FITC^+$ and $FITC^-$ fractions, suggesting that FTY720 inhibited the emigration of SP thymocytes regardless of FITC labeling (Fig. 6 A). These effects coincided with the barely detectable levels of CD4 and CD8 SP $FITC^+$ cells in the blood circulation of FTY720-treated mice (Fig. 6 B).

Consistent with previous results (8), $FITC^+$ cells were detected in the secondary lymphoid organs (such as the MLN) in mock-treated control mice (Fig. 6 C). The positive fraction mainly consisted of cells expressing CD4 or CD8αβ, but not DN or DP cells (Fig. 6 C). The group of mice treated with FTY720 possessed barely detectable levels of $FITC^+$ cells (Fig. 6 C), which was plausibly caused by the inhibition of SP thymocyte emigration by FTY720. These findings led us to conclude that the pathway from the thymus into the MLN is regulated by S1P.

$FITC^+$ cells were found in the large intestine of mock-treated control mice (Fig. 6 D). In FTY720-treated mice, a similar percentage of $FITC^+$ cells was observed, but the absolute $FITC^+$ cell number was decreased because of the reduction in total cell numbers in large intestinal IELs (Figs. 1 A and 6 D). Flow cytometric analysis revealed that $FITC^+$ cells were comprised of DN cells in addition to cells expressing either CD8α or CD4, and that they did not contain any DP cells (Fig. 6 D). As with $FITC^+$ CD4 and CD8α cells in the MLN (Fig. 6 C), FTY720 treatment inhibited the trafficking of $FITC^+$ cells expressing CD4 or CD8α into the large intestine, but did not influence the migration of DN cells (Fig. 6 D). As recent studies have revealed unconventional CD8αα IEL precursors in the DN thymocytes (6, 7, 12), we analyzed TCR expression to reveal that $FITC^+$ DN cells expressed TCRαβ (10–20%) or TCRγδ (10–20%; Fig. 6 D). We also found that $FITC^+$ DN cells barely expressed c-kit, but 50–60% of $FITC^+$ DN cells expressed CD11b and/or CD11c, suggesting that they were phagocytic cells taking up leaked FITC or FITC-labeled apoptotic cells (Fig. 6 D). In addition, $FITC^+$ TCR^+ DN cells were not detected when the same amount of FITC was injected intravenously (unpublished data), excluding a possibility that the $FITC^+$ TCR^+ DN cells observed in this experiment were labeled in the extrathymic compartments. These findings indicate that some $FITC^+$ DN cells are derived from phagocytic cells, whereas others are composed exclusively of cells expressing TCRαβ or TCRγδ. In agreement with these findings, considerable numbers of DN cells expressing TCRαβ or TCRγδ were detected in the blood of FTY720-treated mice, although FTY720 significantly reduced CD4 and CD8 SP cells in the blood (Fig. S3 C). These data suggest that thymic CD4 and CD8 SP cells migrate into the large intestine via an S1P-mediated pathway, and DN cells expressing TCRαβ or TCRγδ migrate via FTY720-insensitive manner.

As one might expect based on the data summarized in Fig. 1, the number of $FITC^+$ cells in the small intestine remained similar after FTY720 treatment (Fig. 6 E), and the $FITC^+$ cells in the small intestine of mock-treated control mice were comprised of DP and DN cells, as well as cells expressing either CD4 or CD8α (Fig. 6 E). Because $CD4^+$ cells exclusively expressed TCRαβ and no cells expressed CD4 together with CD8β in the $FITC^+$ fraction, it seems that DP IELs are $TCR\alpha\beta^+CD8\alpha\alpha^+$ CD4 cells uniquely observed in the intestinal epithelium, and are not thymic DP cells (Fig. 6 E). Small intestinal $FITC^+$ DN IELs included cells expressing CD11b and/or CD11c (~30%), TCRαβ (20–30%), or TCRγδ (30–40%) and few cells expressing c-kit or IL-7R (Fig. 6 E). Like the large intestine, $FITC^+$ TCR^+ DN cells were not detected when the same amount of FITC was injected intravenously (unpublished data). These findings suggest that, similar to the large intestine, some small intestinal $FITC^+$ DN cells are derived from phagocytic cells, whereas others are composed exclusively of cells expressing TCRαβ or TCRγδ, and not cells derived from TCR-negative DN (triple-negative [TN]) cells.

Intriguingly, the ratio of CD8α to CD4 cells was higher in the small intestine than in MLN or the large intestine (Fig. 6, C and D). Those CD8α $FITC^+$ IELs were composed of CD8αα IELs (75%) and CD8αβ IELs (25%; Fig. 6 E), the latter of which expressed CD103, which is a recently reported identifying characteristic of RTEs (Fig. 6 E) (8, 31). FTY720 significantly inhibited the migration of CD4 cells into the small intestine (mock, 4.3 ± 0.35%; FTY720, 1.1 ± 0.23%; $P = 0.009$), whereas other populations including TCRαβ DN cells, TCRγδ DN cells, and $CD103^+$ CD8αβ RTEs were unaffected (Fig. 6 E).

Collectively, our current findings demonstrate that thymic DN IEL precursors expressing TCRαβ or TCRγδ are likely to migrate into the large or small intestine, whereas RTEs preferentially migrate into the small intestine (Fig. 7). Unlike S1P-dependent SP thymocytes' migration into the intestine through secondary lymphoid organs, the migration pathway of unconventional IEL precursors is totally insensitive to FTY720 treatment (Fig. 7).

DISCUSSION

In this study, we demonstrate that the lipid mediator S1P determines whether a given type of IEL goes into the small or the large intestine, resulting in varying proportions of naive cells, RTEs, and thymic DN IEL precursors in the two compartments. Naive IELs, which primarily express $S1P_1$, are more abundant in the large intestine than in the small intestine (Fig. 3 A), explaining why large intestinal IELs are more sensitive to FTY720 or DOP (Figs. 1, 3, and 5). These findings confirm previous reports that identify $CD62L^+$ cells as the primary targets of FTY720 in systemic immunity, and show that $S1P_1$ is preferentially expressed on naive and central memory T cells rather than activated T cells for efficient S1P-mediated migration (18, 32, 33). In contrast, activated IELs, which were abundant in the small intestine but barely detectable in the large intestine, did not respond to FTY720 (Figs. 3 and 4). In this context, a previous study demonstrated that the activation marker CD69 itself induced down-regulation of $S1P_1$, thereby rendering activated cells unresponsive to S1P (34). These findings offer a plausible explanation for why activated IELs expressing CD69 in the intestinal compartments are less reactive to FTY720 (Fig. 3 B).

Our results imply that FTY720 inhibits not only the trafficking of naive IELs into the intestine, but also their retention in the intestinal epithelium (Fig. 4 and Fig. S3). This might explain why naive T cells accumulated in the SLN of FTY720-treated mice, despite their reduced migration from the blood into the SLN (Figs. 2 E and 4 C). A previous work has demonstrated that lymphocyte exit from the skin is not a random process, but is regulated by a chemokine-mediated pathway (35). Additionally, we recently reported that S1P regulates B cell retention in the peritoneal cavity (24). Our current study therefore not only confirms that lymphocyte trafficking in nonlymphoid tissues is regulated biologically, but also shows that S1P plays an important role in that pathway.

In contrast to the S1P-dependent trafficking of naive cells into the intestines through secondary lymphoid organs, thymic DN IEL precursors migrate into both the small and large intestines in an FTY720-insensitive manner (Fig. 6). Recently, several lines of evidence have proposed the presence of IEL precursors in DN thymocytes, including $TCR\alpha\beta^+$ DN thymocytes, $TCR\gamma\delta^+$ DN thymocytes, and $TCR\alpha\beta^-$ $CD25^+$ TN thymocytes (6, 7, 12). $TCR\alpha\beta^+$ DN thymocytes are known as mature post-selected DN thymocytes, as they arise from $CD8\alpha\alpha^+$ $CD4^+$ $CD8\alpha\beta^+$ triple-positive (TP) thymocytes after agonist selection (6). $TCR\alpha\beta^+$ DN thymocytes then migrate into the intestine, where they reinduce $CD8\alpha\alpha$ under the influence of IL-15 (6). It has been shown that TN thymocytes emigrate from the thymus into the intestinal epithelium, where they characteristically express c-kit and IL-7R on the cell surface and mRNA encoding CD3ε (7). This study demonstrates that $FITC^+$ thymic IEL precursors in the intestine of FTY720-treated mice express either TCRαβ or TCRγδ, but not c-kit and IL-7R (Fig. 6, D and E). Thus, although it remains to be determined whether other $CD8\alpha\alpha$ IEL-generating pathways (such as the cryptopatch-dependent route) are dependent on S1P (11) and whether FTY720-resistant S1P-mediated pathways (e.g., $S1P_2$-mediated pathway) are involved in the trafficking of DN thymocytes into the intestines (21), our findings suggest that mature post-selected $TCR\alpha\beta^+$ DN thymocytes and $TCR\gamma\delta^+$ DN thymocytes, but not TN thymocytes, migrate into the gut in a FTY720-insensitive manner.

In addition to thymic DN IEL precursors, the migration of RTEs from the thymus into the small intestine was not inhibited by FTY720 treatment (Fig. 6 E). It has been shown that RTEs uniquely express α4β7 integrin and CCR9 in the thymus, which enables them to migrate directly into the small intestinal epithelium without undergoing activation in the secondary lymphoid organs (8). Their preferential migration into the small intestine rather than the large intestine can be explained by their CCR9 expression in the thymus, as small intestinal ECs, unlike those of the large intestine, produce an abundance of the CCR9 ligand CCL25 (28). Our current data indicate that FTY720 does not affect the direct migration of RTEs from the thymus into the small intestine. Although FTY720 had no effect on RTEs, which were known to express CD62L (8), naive $CD62L^{high}$ cells were barely detected in the small intestine of FTY720-treated mice (<0.1%; Fig. 3 A). This discrepancy is caused by the fact that the RTEs are very minor population in the small intestinal IELs. In this issue, it was previously demonstrated that ~2% of cells were RTEs in $CD62L^{high}CD44^{int}$ $CD8\alpha\beta$ cells, which consisted of 5% small intestinal $CD8\alpha\beta$ IELs (8). Therefore, an estimated percentage of RTEs in the total small intestinal IELs, including CD4, $CD8\alpha\alpha$, $CD8\alpha\beta$, and DN cells, is <0.1%. Thus, it is likely that the RTEs are present, but difficult to detect, in the small intestine of FTY720-treated mice. Additionally, there is still a minor possibility of the involvement of other cells that express CD103, CD62L, and CCR9 (e.g., circulating naive CD8 T cells and SP CD8 thymocytes). However, together with well-established effects of FTY720 on circulating naive CD8 T cells and SP CD8 thymocytes on their retention in the secondary lymphoid organs and thymus (16, 17) and our data on FITC-labeling experiments, the most plausible interpretation is that RTEs use the unique FTY720-insensitive trafficking pathway from the thymus into the small intestinal epithelium.

In addition to activated platelets, mast cells, and monocytes, dietary sphingolipids are another source of S1P (36). Interestingly, enzymes involved in the generation of sphingosine, which is a precursor of S1P, are principally expressed in the intestinal tracts, where their expression patterns differ

according to the intestinal compartment (37, 38). For instance, alkaline sphingomyelinase and neutral ceramidase, which are both important enzymes in the sequential degradation of sphingomyelin and ceramide to generate sphingosine, were predominantly expressed at the luminal side of the brush border in the distal jejunum and ileum, indicating that the amount of sphingosine was much lower in the upper and middle sections than in the lower sections of the small and large intestines (37, 38). The varying expression patterns of these enzymes, which might determine to what degree IELs migrate into a given region of the small or large intestine, depend on S1P under natural conditions. Although FTY720 inhibits the naive cell trafficking into the intestinal epithelium by preventing their emigration from the secondary lymphoid organs in our experimental condition (Fig. 2 E), it is interesting to examine whether luminal sphingosine-derived S1P regulates intestinal immunity, including T cell trafficking. Studies are currently underway in our group to further investigate this issue.

As S1P mediates the migration of mucosal T cells, such as IELs, it might also regulate other groups of immunocompetent and/or pathological cells in the mucosal immune system. Most irritations of the gastrointestinal tract, including inflammatory bowel diseases (IBDs) and food allergies, are caused by the influx of pathological cells into the intestine from systemic compartments (39, 40). If the migration of these pathological cells to the gastrointestinal tract is indeed S1P-dependent, it should be susceptible to FTY720, perhaps opening a new avenue for the treatment of IBDs and intestinal allergic diseases. Indeed, our previous study demonstrated that FTY720 effectively inhibited the development of IBDs in IL-10–deficient mice (41). Moreover, our recent separate studies show that FTY720 is also effective at preventing the development of allergic diarrhea by inhibiting pathogenic cell migration into the large intestine (42). In addition to regulating IEL trafficking under natural conditions, these findings suggest that the S1P-mediated pathway is involved in the development of immunological diseases of the intestine, such as IBDs and food allergies.

MATERIALS AND METHODS

Mice and experimental treatment. Normal female BALB/c mice (7–9 wk of age) were purchased from Japan Clea or Japan SLC. All mice were provided with sterile food and water ad libitum. Mice were injected intraperitoneally with 1 mg/kg FTY720 (Novartis Pharma) to assess reactivity (18, 24). To inhibit S1P lyase activity, the mice received drinking water containing 10 g/liter glucose and 30 mg/liter 4-deoxypyridoxine-HCl (Sigma-Aldrich) for 3 d (23). All animals were maintained in the experimental animal facility at the University of Tokyo, and the experiments were conducted in accordance with the guidelines provided by the Animal Care and Use Committee of the University of Tokyo.

Lymphocyte isolation. Single IEL cells were isolated from the small and large intestinal epithelium as previously described (43). In brief, after removing the PPs, the small and large intestines were dissected into short segments and stirred at 37°C in prewarmed RPMI 1640 containing 2% FCS and 0.5 mM EDTA for 15 min, followed by vigorous shaking for 15 s. This process was repeated twice. A discontinuous Percoll density gradient centrifugation was performed to purify the lymphocytes. IELs were collected from the layer between the 40% and 75% fractions. The spleen, thymus, MLN, SLN, PPs, and CPs were removed, and single-cell suspensions were prepared by passing them through a 70-μm mesh filter, as previously described (24, 44). Lymphocytes were prepared from the liver according to a previously established method (45). In brief, the liver was passed through a 200-gauge stainless mesh to obtain single cells. These cells were treated with erythrocyte-lysing solution (155 mM NH_4Cl, 10 mM $KHCO_3$, 1 mM EDTA, and 170 mM Tris-HCl, pH 7.3) to remove the erythrocytes, and were then fractionated by centrifugation in 35% Percoll.

Flow cytometry and cell sorting. Flow cytometry and cell sorting were performed as previously described (24, 44). Cells were preincubated with anti-CD16/32 antibody, and then stained with fluorescent antibodies specific for CD4, CD8α, CD8β, CD11b, CD11c, CD44, CD62L, CD69, CD103, c-kit, IL-7R, TCRβ, TCRγδ, α4β7 integrin (BD PharMingen), and CCR9 (R&D Systems). A Viaprobe (BD PharMingen) was used to discriminate between dead and living cells. Flow-cytometric analysis and cell sorting were performed using FACSCalibur and FACSAria (BD Biosciences), respectively.

Histological analysis. Immunohistochemical analysis was performed as previously described (40). In brief, large intestines were fixed in 4% paraformaldehyde (Wako) and treated with a sucrose gradient after extensive washing. The tissue was embedded in Tissue-Tek OCT compound (Sakura Finetechnical). For confocal microscopy analysis, TSA-direct kit (Perkin Elmer) was used according to the manufacturer's instructions. In brief, 6-μm cryostat sections were treated with 3% H_2O_2 in PBS for 15 min to quench endogenous peroxidase activity. Sections were preblocked with anti-CD16/CD32 antibody in PBS containing 2% FCS for 15 min at room temperature, and stained with biotin-conjugated antibodies specific for CD4 or CD62L for 15 h at 4°C. After washing with TNT buffer (0.1 M Tris-HCl, pH 7.5, 0.15 M NaCl, and 0.05% Tween20), sections were treated with horseradish peroxidase–conjugated streptavidin in TNT buffer for 30 min at room temperature. After washing with TNT buffer, amplification of the fluorescent signal with FITC or Cy5-tyramide was performed. The specimens were analyzed using a confocal laser-scanning microscope (TCS SP2; Leica). Hematoxylin and eosin staining was used to confirm the dissociation of the epithelial region, as previously described (40)

Quantitative RT-PCR. To measure mRNA expression for S1P receptors, quantitative RT-PCR using LightCycler (Roche) was performed as previously described (24). Total RNA was prepared using TRIzol reagent (Invitrogen), and cDNA was synthesized using Powerscript reverse transcriptase (BD Biosciences). The oligonucleotide primers and probes specific for $S1P_1$ (forward primer, TACACTCTGACCAACAAGGA; reverse primer, ATAATGGTCTCTGGGTTGTC;FITC-probe,TGCTGGCAATTCAAGAGGCCCATCATC; and LCRed 640-probe, CAGGCATGGAATTTAGCCGCAGCAAATC) and GAPDH (forward primer, TGAACGGGAAGCTCACTGG; reverse primer, TCCACCACCCTGTTGCTGTA; FITC-probe, CTGAGGACCAGGTTGTCTCCTGCGA; and LCRed 640-probe, TTCAACAGCAACTCCCACTCTTCCACC) were designed and produced by Nihon Gene Research Laboratory.

Adoptive transfer of CFSE-labeled lymphocytes. $CD3^+$ T cells were isolated from the MLN and SLN using anti–mouse CD3-coupled microbeads and a MACS column (Miltenyi Biotec) as previously described (44). For CFSE labeling, 10^7 cells were incubated in the dark with 10 μM CFSE (Invitrogen) for 10 min at 37°C, before being washed twice with PBS (8, 24). Labeled cells (2×10^7) were adoptively transferred via the tail vein into naive mice, which were either treated with FTY720 5 min after the cell transfer or left untreated. Lymphocytes were isolated from the MLN, SLN, blood, PPs, and small and large intestinal epithelium 24 h and 7 d after the transfer for flow-cytometric analysis.

Intrathymic labeling of thymocytes with FITC. The intrathymic injection of FITC was performed as previously described (8, 22, 31). In brief, 10 μl FITC solution (1 mg/ml; Sigma-Aldrich) was injected into the thymus of anesthetized mice and the skin was closed with silk sutures. For FTY720 treatment, the mice were treated with FTY720 5 min before the FITC injection. Lymphocytes were isolated from the thymus, blood, MLN, and small and large intestinal epithelium 24 h after the FITC injection for flow-cytometric analysis.

BrdU incorporation and measurement. Mice were injected intraperitoneally with 1 mg BrdU (Sigma-Aldrich) in PBS as previously described (46). At the indicated times, the IELs were isolated from the small and large intestines and stained with fluorescent antibodies specific for CD4 and CD62L (BD PharMingen). BrdU incorporation was detected by flow cytometry with a BrdU Flow kit according to the manufacturer's instructions (BD Biosciences).

Statistics. Results were compared using the Student's or Welch's *t* test. Statistical significance was established at $P < 0.05$.

Online supplemental material. Fig. S1 shows the data on CD4 and CD8 cells in the thymus, spleen, liver, PPs, CPs, and lymphocyte aggregates of mice treated with FTY720. Fig. S2 provides the data on the CCR9 expression on small and large intestinal CD8 IELs. Fig. S3 shows data on FACS profile in the PPs of FTY720-treated mice, naive T cells cultured with FTY720, and cell numbers of blood lymphocytes of FTY720-treated mice. The online version of this article is available at http://www.jem.org/cgi/content/full/jem.20062446/DC1.

We thank Y. Takahama for helpful discussions and technical advice and K. McGhee for editorial help.

This work was supported by grants from Core Research for Evolutional Science and Technology of the Japan Science and Technology Corporation; the Ministry of Education, Science, Sports, and Culture; the Ministry of Health and Welfare in Japan; the Waksman Foundation of Japan; and Yakult Bio-Science Foundation.

The authors have no conflicting financial interests.

Submitted: 21 November 2006
Accepted: 15 August 2007

REFERENCES

1. Kiyono, H., and S. Fukuyama. 2004. NALT- versus Peyer's-patch-mediated mucosal immunity. *Nat. Rev. Immunol.* 4:699–710.
2. Kunisawa, J., and H. Kiyono. 2005. A marvel of mucosal T cells and secretory antibodies for the creation of first lines of defense. *Cell. Mol. Life Sci.* 62:1308–1321.
3. Kunisawa, J., S. Fukuyama, and H. Kiyono. 2005. Mucosa-associated lymphoid tissues in aerodigestive tract: their shared and divergent traits and their importance to the orchestration of mucosal immune system. *Curr. Mol. Med.* 5:557–572.
4. Kunisawa, J., I. Takahashi, and H. Kiyono. 2007. Intraepithelial lymphocytes: their shared and divergent immunological behaviors in the small and large intestine. *Immunol. Rev.* 215:136–153.
5. Cheroutre, H. 2004. Starting at the beginning: new perspectives on the biology of mucosal T cells. *Annu. Rev. Immunol.* 22:217–246.
6. Gangadharan, D., F. Lambolez, A. Attinger, Y. Wang-Zhu, B.A. Sullivan, and H. Cheroutre. 2006. Identification of pre- and post-selection TCR$\alpha\beta^+$ intraepithelial lymphocyte precursors in the thymus. *Immunity.* 25:631–641.
7. Lambolez, F., M.L. Arcangeli, A.M. Joret, V. Pasqualetto, C. Cordier, J.P. Di Santo, B. Rocha, and S. Ezine. 2006. The thymus exports long-lived fully committed T cell precursors that can colonize primary lymphoid organs. *Nat. Immunol.* 7:76–82.
8. Staton, T.L., A. Habtezion, M.M. Winslow, T. Sato, P.E. Love, and E.C. Butcher. 2006. CD8$^+$ recent thymic emigrants home to and efficiently repopulate the small intestine epithelium. *Nat. Immunol.* 7:482–488.
9. Eberl, G., and D.R. Littman. 2004. Thymic origin of intestinal $\alpha\beta$ T cells revealed by fate mapping of RORγt+ cells. *Science.* 305:248–251.
10. Guy-Grand, D., O. Azogui, S. Celli, S. Darche, M.C. Nussenzweig, P. Kourilsky, and P. Vassalli. 2003. Extrathymic T cell lymphopoiesis: ontogeny and contribution to gut intraepithelial lymphocytes in athymic and euthymic mice. *J. Exp. Med.* 197:333–341.
11. Saito, H., Y. Kanamori, T. Takemori, H. Nariuchi, E. Kubota, H. Takahashi-Iwanaga, T. Iwanaga, and H. Ishikawa. 1998. Generation of intestinal T cells from progenitors residing in gut cryptopatches. *Science.* 280:275–278.
12. Pennington, D.J., B. Silva-Santos, and A.C. Hayday. 2005. $\gamma\delta$ T cell development–having the strength to get there. *Curr. Opin. Immunol.* 17:108–115.
13. Beagley, K.W., K. Fujihashi, A.S. Lagoo, S. Lagoo-Deenadaylan, C.A. Black, A.M. Murray, A.T. Sharmanov, M. Yamamoto, J.R. McGhee, C.O. Elson, et al. 1995. Differences in intraepithelial lymphocyte T cell subsets isolated from murine small versus large intestine. *J. Immunol.* 154:5611–5619.
14. Camerini, V., C. Panwala, and M. Kronenberg. 1993. Regional specialization of the mucosal immune system. Intraepithelial lymphocytes of the large intestine have a different phenotype and function than those of the small intestine. *J. Immunol.* 151:1765–1776.
15. Ibraghimov, A.R., and R.G. Lynch. 1994. Heterogeneity and biased T cell receptor α/β repertoire of mucosal CD8$^+$ cells from murine large intestine: implications for functional state. *J. Exp. Med.* 180:433–444.
16. Rosen, H., and E.J. Goetzl. 2005. Sphingosine 1-phosphate and its receptors: an autocrine and paracrine network. *Nat. Rev. Immunol.* 5:560–570.
17. Cyster, J.G. 2005. Chemokines, sphingosine-1-phosphate, and cell migration in secondary lymphoid organs. *Annu. Rev. Immunol.* 23: 127–159.
18. Matloubian, M., C.G. Lo, G. Cinamon, M.J. Lesneski, Y. Xu, V. Brinkmann, M.L. Allende, R.L. Proia, and J.G. Cyster. 2004. Lymphocyte egress from thymus and peripheral lymphoid organs is dependent on S1P receptor 1. *Nature.* 427:355–360.
19. Allende, M.L., J.L. Dreier, S. Mandala, and R.L. Proia. 2004. Expression of the sphingosine 1-phosphate receptor, $S1P_1$, on T-cells controls thymic emigration. *J. Biol. Chem.* 279:15396–15401.
20. Graler, M.H., and E.J. Goetzl. 2004. The immunosuppressant FTY720 down-regulates sphingosine 1-phosphate G-protein-coupled receptors. *FASEB J.* 18:551–553.
21. Mandala, S., R. Hajdu, J. Bergstrom, E. Quackenbush, J. Xie, J. Milligan, R. Thornton, G.J. Shei, D. Card, C. Keohane, et al. 2002. Alteration of lymphocyte trafficking by sphingosine-1-phosphate receptor agonists. *Science.* 296:346–349.
22. Yagi, H., R. Kamba, K. Chiba, H. Soga, K. Yaguchi, M. Nakamura, and T. Itoh. 2000. Immunosuppressant FTY720 inhibits thymocyte emigration. *Eur. J. Immunol.* 30:1435–1444.
23. Schwab, S.R., J.P. Pereira, M. Matloubian, Y. Xu, Y. Huang, and J.G. Cyster. 2005. Lymphocyte sequestration through S1P lyase inhibition and disruption of S1P gradients. *Science.* 309:1735–1739.
24. Kunisawa, J., Y. Kurashima, M. Gohda, M. Higuchi, I. Ishikawa, F. Miura, I. Ogahara, and H. Kiyono. 2007. Sphingosine 1-phosphate regulates peritoneal B cell trafficking for subsequent intestinal IgA production. *Blood.* 109:3749–3756.
25. Chiba, K., Y. Yanagawa, Y. Masubuchi, H. Kataoka, T. Kawaguchi, M. Ohtsuki, and Y. Hoshino. 1998. FTY720, a novel immunosuppressant, induces sequestration of circulating mature lymphocytes by acceleration of lymphocyte homing in rats. I. FTY720 selectively decreases the number of circulating mature lymphocytes by acceleration of lymphocyte homing. *J. Immunol.* 160:5037–5044.
26. Wagner, N., J. Lohler, E.J. Kunkel, K. Ley, E. Leung, G. Krissansen, K. Rajewsky, and W. Muller. 1996. Critical role for β7 integrins in formation of the gut-associated lymphoid tissue. *Nature.* 382:366–370.
27. Cepek, K.L., S.K. Shaw, C.M. Parker, G.J. Russell, J.S. Morrow, D.L. Rimm, and M.B. Brenner. 1994. Adhesion between epithelial cells and T lymphocytes mediated by E-cadherin and the $\alpha E\beta 7$ integrin. *Nature.* 372:190–193.

28. Kunkel, E.J., J.J. Campbell, G. Haraldsen, J. Pan, J. Boisvert, A.I. Roberts, E.C. Ebert, M.A. Vierra, S.B. Goodman, M.C. Genovese, et al. 2000. Lymphocyte CC chemokine receptor 9 and epithelial thymus-expressed chemokine (TECK) expression distinguish the small intestinal immune compartment: epithelial expression of tissue-specific chemokines as an organizing principle in regional immunity. *J. Exp. Med.* 192:761–768.
29. Halin, C., M.L. Scimone, R. Bonasio, J.M. Gauguet, T.R. Mempel, E. Quackenbush, R.L. Proia, S. Mandala, and U.H. von Andrian. 2005. The S1P-analog FTY720 differentially modulates T-cell homing via HEV: T-cell-expressed $S1P_1$ amplifies integrin activation in peripheral lymph nodes but not in Peyer patches. *Blood.* 106:1314–1322.
30. Lefrancois, L., C.M. Parker, S. Olson, W. Muller, N. Wagner, M.P. Schon, and L. Puddington. 1999. The role of β7 integrins in CD8 T cell trafficking during an antiviral immune response. *J. Exp. Med.* 189:1631–1638.
31. Staton, T.L., B. Johnston, E.C. Butcher, and D.J. Campbell. 2004. Murine $CD8^+$ recent thymic emigrants are αE integrin-positive and CC chemokine ligand 25 responsive. *J. Immunol.* 172:7282–7288.
32. Bohler, T., J. Waiser, M. Schuetz, H.H. Neumayer, and K. Budde. 2004. FTY720 exerts differential effects on $CD4^+$ and $CD8^+$ T-lymphocyte subpopulations expressing chemokine and adhesion receptors. *Nephrol. Dial. Transplant.* 19:702–713.
33. Graeler, M., and E.J. Goetzl. 2002. Activation-regulated expression and chemotactic function of sphingosine 1-phosphate receptors in mouse splenic T cells. *FASEB J.* 16:1874–1878.
34. Shiow, L.R., D.B. Rosen, N. Brdickova, Y. Xu, J. An, L.L. Lanier, J.G. Cyster, and M. Matloubian. 2006. CD69 acts downstream of interferon-α/β to inhibit $S1P_1$ and lymphocyte egress from lymphoid organs. *Nature.* 440:540–544.
35. Debes, G.F., C.N. Arnold, A.J. Young, S. Krautwald, M. Lipp, J.B. Hay, and E.C. Butcher. 2005. Chemokine receptor CCR7 required for T lymphocyte exit from peripheral tissues. *Nat. Immunol.* 6:889–894.
36. Vesper, H., E.M. Schmelz, M.N. Nikolova-Karakashian, D.L. Dillehay, D.V. Lynch, and A.H. Merrill Jr. 1999. Sphingolipids in food and the emerging importance of sphingolipids to nutrition. *J. Nutr.* 129:1239–1250.
37. Duan, R.D., L. Nyberg, and A. Nilsson. 1995. Alkaline sphingomyelinase activity in rat gastrointestinal tract: distribution and characteristics. *Biochim. Biophys. Acta.* 1259:49–55.
38. Kono, M., J.L. Dreier, J.M. Ellis, M.L. Allende, D.N. Kalkofen, K.M. Sanders, J. Bielawski, A. Bielawska, Y.A. Hannun, and R.L. Proia. 2006. Neutral ceramidase encoded by the Asah2 gene is essential for the intestinal degradation of sphingolipids. *J. Biol. Chem.* 281:7324–7331.
39. Powrie, F., M.W. Leach, S. Mauze, S. Menon, L.B. Caddle, and R.L. Coffman. 1994. Inhibition of Th1 responses prevents inflammatory bowel disease in scid mice reconstituted with $CD45RB^{hi}$ $CD4^+$ T cells. *Immunity.* 1:553–562.
40. Kweon, M.N., M. Yamamoto, M. Kajiki, I. Takahashi, and H. Kiyono. 2000. Systemically derived large intestinal $CD4^+$ Th2 cells play a central role in STAT6-mediated allergic diarrhea. *J. Clin. Invest.* 106:199–206.
41. Mizushima, T., T. Ito, D. Kishi, Y. Kai, H. Tamagawa, R. Nezu, H. Kiyono, and H. Matsuda. 2004. Therapeutic effects of a new lymphocyte homing reagent FTY720 in interleukin-10 gene-deficient mice with colitis. *Inflamm. Bowel Dis.* 10:182–192.
42. Kurashima, Y., J. Kunisawa, M. Higuchi, M. Gohda, I. Ishikawa, N. Takayama, M. Shimizu, and H. Kiyono. 2007. Sphingosine 1-phosphate-mediated trafficking of pathogenic Th2 and mast cells for the control of food allergy. *J. Immunol.* 179:1577–1585.
43. Kinoshita, N., T. Hiroi, N. Ohta, S. Fukuyama, E.J. Park, and H. Kiyono. 2002. Autocrine IL-15 mediates intestinal epithelial cell death via the activation of neighboring intraepithelial NK cells. *J. Immunol.* 169:6187–6192.
44. Kunisawa, J., T. Nakanishi, I. Takahashi, A. Okudaira, Y. Tsutsumi, K. Katayama, S. Nakagawa, H. Kiyono, and T. Mayumi. 2001. Sendai virus fusion protein mediates simultaneous induction of MHC class I/II-dependent mucosal and systemic immune responses via the nasopharyngeal-associated lymphoreticular tissue immune system. *J. Immunol.* 167:1406–1412.
45. Kato, T., Y. Sato, S. Takahashi, H. Kawamura, K. Hatakeyama, and T. Abo. 2004. Involvement of natural killer T cells and granulocytes in the inflammation induced by partial hepatectomy. *J. Hepatol.* 40:285–290.
46. Penney, L., P.J. Kilshaw, and T.T. MacDonald. 1995. Regional variation in the proliferative rate and lifespan of $\alpha\beta$ TCR^+ and $\gamma\delta$ TCR^+ intraepithelial lymphocytes in the murine small intestine. *Immunology.* 86:212–218.

A novel M cell–specific carbohydrate-targeted mucosal vaccine effectively induces antigen-specific immune responses

Tomonori Nochi,[1,3] Yoshikazu Yuki,[1,3] Akiko Matsumura,[1,3] Mio Mejima,[1,3] Kazutaka Terahara,[1,3] Dong-Young Kim,[1,3] Satoshi Fukuyama,[1,3] Kiyoko Iwatsuki-Horimoto,[2,3] Yoshihiro Kawaoka,[2,3] Tomoko Kohda,[4] Shunji Kozaki,[4] Osamu Igarashi,[1,3] and Hiroshi Kiyono[1,3]

[1]Division of Mucosal Immunology, [2]Division of Virology, The Institute of Medical Science, The University of Tokyo, Tokyo 108-8639, Japan
[3]Core Research for Evolutional Science and Technology, Japan Science and Technology Corporation, Saitama 332-0012, Japan
[4]Laboratory of Veterinary Epidemiology, Department of Veterinary Science, Graduate School of Life and Environmental Sciences, Osaka Prefecture University, Osaka 599-8531, Japan

Mucosally ingested and inhaled antigens are taken up by membranous or microfold cells (M cells) in the follicle-associated epithelium of Peyer's patches or nasopharynx-associated lymphoid tissue. We established a novel M cell–specific monoclonal antibody (mAb NKM 16-2-4) as a carrier for M cell–targeted mucosal vaccine. mAb NKM 16-2-4 also reacted with the recently discovered villous M cells, but not with epithelial cells or goblet cells. Oral administration of tetanus toxoid (TT)– or botulinum toxoid (BT)–conjugated NKM 16-2-4, together with the mucosal adjuvant cholera toxin, induced high-level, antigen-specific serum immunoglobulin (Ig) G and mucosal IgA responses. In addition, an oral vaccine formulation of BT-conjugated NKM 16-2-4 induced protective immunity against lethal challenge with botulinum toxin. An epitope analysis of NKM 16-2-4 revealed specificity to an α(1,2)-fucose–containing carbohydrate moiety, and reactivity was enhanced under sialic acid–lacking conditions. This suggests that NKM 16-2-4 distinguishes α(1,2)-fucosylated M cells from goblet cells containing abundant sialic acids neighboring the α(1,2) fucose moiety and from non-α(1,2)-fucosylated epithelial cells. The use of NKM 16-2-4 to target vaccine antigens to the M cell–specific carbohydrate moiety is a new strategy for developing highly effective mucosal vaccines.

CORRESPONDENCE
Hiroshi Kiyono:
kiyono@ims.u-tokyo.ac.jp

Membranous or microfold cells (M cells), which are located in the follicle-associated epithelium (FAE) of Peyer's patches (PPs) or nasopharynx-associated lymphoid tissue (NALT), play a pivotal role in the uptake of luminal antigens for induction of antigen-specific immune responses in both systemic and mucosal compartments (1). Unlike their neighboring columnar epithelial cells, M cells are morphologically unique because they have irregular and short microvilli for the effective uptake of ingested or inhaled antigens from luminal sites in the aerodigestive tract; they subsequently transport the sampled antigen to professional antigen-presenting cells (e.g., dendritic cells) to initiate antigen sensitization (2).

The mucosal immune system consists of two types of immunologically important sites, termed "inductive" and "effector" tissues, connected by the common mucosal immune system (3). In general, antigen sensitization occurs at inductive sites, such as PPs, after antigen uptake by M cells. Induction of antigen-specific T helper 2 (Th2) cell–mediated IgA responses and Th1 cell– and CTL-dependent immune responses then occurs at effector sites such as the lamina propria (3). However, our recent study demonstrated that the effector sites are also able to take up antigen, because antigen-sampling cells termed villous M cells are distributed in the intestinal villous epithelium (4), and antigen-specific mucosal immune responses can be induced in PP-deficient mice (5).

Although mucosal vaccination is thought to be an ideal strategy for combating mucosal infectious diseases, only a few mucosal vaccines (e.g., polio vaccine and influenza vaccine) are

The online version of this article contains supplemental material.

JEM © The Rockefeller University Press $30.00
Vol. 204, No. 12, November 26, 2007 2789-2796 www.jem.org/cgi/doi/10.1084/jem.20070607

currently used in humans because they have lower efficacy than the currently used injectable vaccines in inducing antigen-specific immune responses (6). Because M cells possess the ability to take up luminal antigens, it is logical and attractive to develop a system of delivery of vaccine antigen to both PP-associated and villous M cells to create an effective mucosal vaccine (7). In fact, *Ulex europaeus* agglutinin-1 (UEA-1)–conjugated (8, 9) or σ1 protein–conjugated nasal vaccination (10, 11) induce not only strong antigen-specific plasma IgG and mucosal IgA responses but also CTL immunity, because UEA-1 specific for α(1,2) fucose specifically reacts with murine PP–associated and villous M cells (4, 12), and σ1 protein derived from reovirus specifically binds to a carbohydrate structure containing α(2,3)-linked sialic acid on the membranes of M cells (13). However, because UEA-1 also reacts strongly with goblet cells and the mucus layer covering the intestinal epithelium (14), there have been no effective oral vaccines with UEA-1 as an M cell–targeting vehicle. To overcome this obstacle, we established an M cell–specific mAb and developed a novel strategy for oral vaccination with high efficacy.

RESULTS AND DISCUSSION

Establishment of an M cell–specific monoclonal antibody (NKM 16-2-4)

To characterize the antigen-sampling M cells for development of an effective M cell–targeted mucosal vaccine, Sprague-Dawley (SD) rats were immunized 4 times at 2-wk intervals with highly purified (>95%) UEA-1–positive cells isolated from murine PPs to establish an M cell–specific mAb. A total of 1,000 hybridomas were generated and screened by immunohistochemical analysis of intestinal tissue sections containing PPs. On the basis of the initial screening, one clone (NKM 16–2-4; rat IgG2c), which possessed specificity to M cells located in the FAE of PPs (Fig. 1 A), was selected. Half of the hybridomas showed no specificity to tissue sections; ~40% of them showed strong reactivity to goblet cells and their secretions; and 10% showed reactivity to the microvilli in all parts of the intestinal epithelium, including M cells and neighboring columnar epithelial cells (unpublished data). These initial screening data indicated that the goblet cells contained in the immunized UEA-1–positive fraction, and their secretions, were vastly immunodominant compared with M cells. However, importantly, NKM 16–2-4 possessed no reactivity to UEA-1–positive goblet cells located in the intestinal villi (Fig. 1 A), indicating that NKM 16–2-4 is a novel mAb possessing high specificity to murine M cells. This is unlike the already known murine M cell–specific lectin UEA-1, which also reacts with goblet cells and their secretions (14). In addition, NKM 16–2-4 reacted very strongly with the apical surfaces of the M cells (Fig. 1 A), rather than the cytoplasm, suggesting that it might be able to be used as a carrier vehicle of M cell–targeted mucosal vaccine. In support of these results, flow cytometric and immuno- and lectin-cytochemical analyses demonstrated that NKM 16–2-4 specifically reacted with the surfaces of isolated UEA-1–positive M cells (Fig. S1, available at http://www.jem.org/cgi/content/full/jem.20070607/DC1), but not of UEA-1–negative epithelial cells. In addition, an electronmicroscopic analysis revealed that NKM 16–2-4 specifically reacted with typical M cells, which have short and irregular microvilli and a pocket structure containing lymphocytes and/or monocytes (Fig. 1 B). Furthermore, whole-mount staining analysis revealed that NKM 16–2-4 specifically reacted with villous M cells, in a manner similar to the reaction with PP-associated M cells (Fig. 1 C).

M cells recognized by UEA-1 in mice are also present in the FAE of NALT, as they are in PPs, and act as antigen-sampling cells for the induction of mucosal immunity (15), although our previous finding demonstrated that the mechanism of NALT organogenesis is distinct from that of PP organogenesis (16, 17). Recently, it was reported that group A streptococcus infects its hosts through M cells (15), meaning that M cells could be defined as a portal cell subset of mucosal infection in both the gastrointestinal and respiratory tracts. A subsequent immunohistochemical analysis of NALT tissue sections revealed that NKM 16–2-4 specifically reacted with UEA-1–positive M cells, but not UEA-1–positive, morphologically typical goblet cells with secretory granules (Fig. S2, available at http://www.jem.org/cgi/content/full/jem.20070607/DC1). These results further suggest the possibility of formulating an M cell–targeted nasal vaccine with NKM 16–2-4 for protection against infectious diseases entering through the respiratory tract. Thus, in summary, the novel mAb NKM 16–2-4 specifically reacted with all subsets of M cells, but not epithelial cells or goblet cells, located in PPs, NALT, and the intestinal villi; i.e., in both the gastrointestinal and respiratory tracts (Table I).

Use of NKM 16–2-4 to develop an M cell–targeted mucosal vaccine

Because it had been reported that the use of monoclonal antibodies to target injectable vaccine antigen to dendritic cells expressing endocytic receptor effectively initiated antigen-specific immunity (18, 19), we next addressed the characteristics of NKM 16–2-4 as a carrier vehicle of M cell–targeted mucosal vaccines. When we injected FITC-conjugated NKM 16–2-4 or FITC-conjugated control rat IgG into intestinal loops containing PPs, FITC-conjugated NKM 16–2-4 specifically attached to the apical surfaces of M cells in the dome regions of PPs within 10 min of inoculation, whereas FITC-conjugated control rat IgG did not (Fig. 2 A). Furthermore, FITC-conjugated NKM 16–2-4 was taken into the cytoplasmic regions of M cells within 30 min (Fig. 2 A) and reached the basal membrane of the M cells within 4 h, indicating that NKM 16–2-4 could likely be used as a carrier vehicle of orally administered vaccine antigen to M cells.

To directly confirm that M cell–targeted mucosal vaccination with NKM 16–2-4 is an effective strategy for inducing high-level, antigen-specific immune responses, tetanus toxoid (TT) was selected as a prototypical vaccine antigen, as TT has been extensively used in our previous experiments to elucidate the mechanism of the antigen-specific immune responses induced in both the mucosal and systemic compartments by mucosal immunization (20). A chimeric complex of

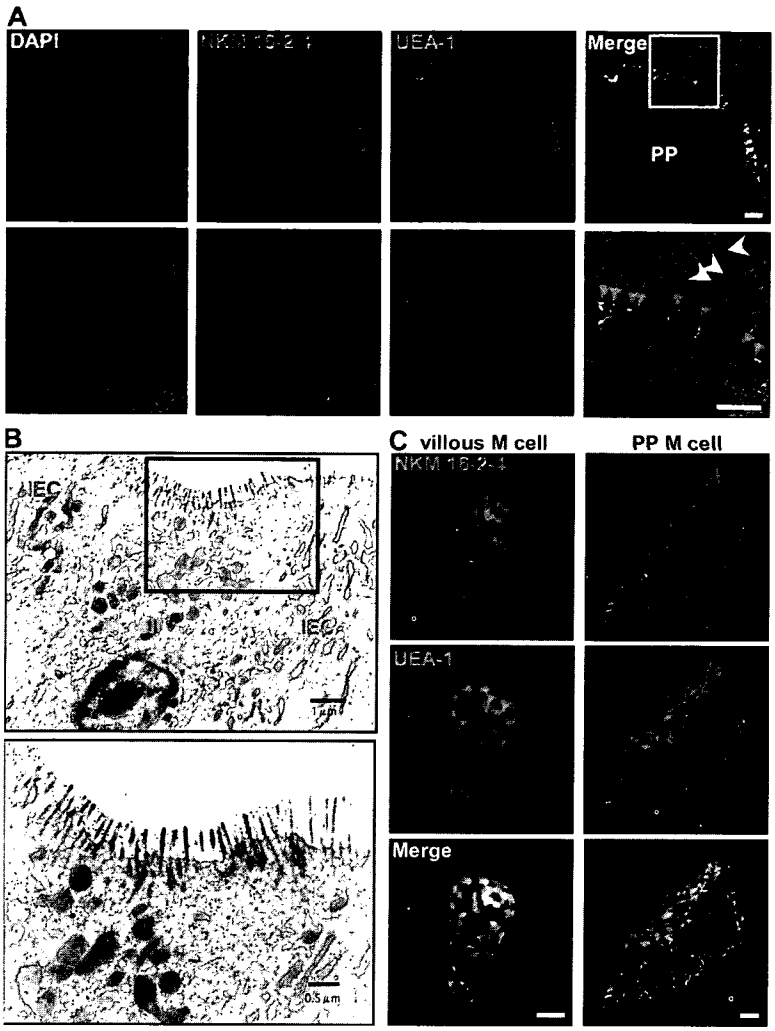

Figure 1. Immunohistochemical analysis for the specificity of NKM 16–2–4. (A) Immunohistochemical analysis of PPs revealed that NKM 16–2–4 specifically reacted with UEA-1–positive M cells (red arrows), but not UEA-1–positive goblet cells (yellow arrowheads). (B) Electronmicroscopic analysis revealed that typical M cells, which had short and irregular microvilli and pocket structures containing lymphocytes and/or monocytes, specifically reacted with NKM 16–2–4. Positive reactions are shown by gold particles (18 nm). IEC, intestinal epithelial cell. (C) Whole-mount staining of PPs and villous epithelium demonstrated that, in addition to PP-associated M cells, UEA-1–positive villous M cells were specifically recognized by NKM 16–2–4. Bars, 50 μm.

TT conjugated with NKM 16–2–4 or control rat IgG (in total, each 200 μg contained 50 μg TT per mouse) was prepared by using avidin–biotin complexes (see Materials and methods). The prepared complexes consisted of TT and NKM 16–2–4 or control rat IgG; these complexes, or noncoupled TT, were orally administered to mice, together with the mucosal adjuvant cholera toxin (CT). In addition, it has been reported that M cell–targeted mucosal vaccine with UEA-1 is effective in inducing antigen-specific humoral and cellular immunity when administered via the nasal route (8, 9); therefore, we prepared an orally administered TT-conjugated UEA-1 as a control for the efficacy of the NKM 16–2–4–based M cell–targeted mucosal vaccines. As expected, brisk TT-specific serum IgG and mucosal IgA responses were induced in mice immunized with TT-conjugated NKM 16–2–4, whereas TT-conjugated control rat IgG or 50 μg noncoupled TT induced, at best, very low TT-specific immune responses (Fig. 2 B). In addition, the level of the TT-specific immune response induced by TT-conjugated UEA-1 was lower than that induced by TT-conjugated NKM 16–2–4. These data suggest that an M cell–targeted mucosal vaccine with UEA-1 might be insufficient for antigen delivery to M cells, because the UEA-1–based vaccine is trapped by goblet cells and their secreting mucus, as well as by M cells. Furthermore, 10 times more noncoupled TT (500 μg) induced a small TT-specific immune response compared with TT-conjugated NKM 16–2–4 containing 50 μg TT (Fig. 2 B), perhaps because of the low efficacy of antigen delivery to M cells for the induction of antigen-specific immune responses. Although the levels of the antigen-specific antibody responses induced here by immunization with noncoupled TT and CT tended to

Table I. Immunological and biochemical characteristics of newly established mAb (NKM 16-2-4) and UEA-1 in M cells

mAb/lectin	Specificity	Cell specificity		
		M cells	Epithelial cells	Goblet cells
NKM 16-2-4	α(1,2) fucose-containing carbohydrate moiety	+	-	-
UEA-1	α(1,2) fucose	+	-	+

be lower than those in a previous study (20), this discrepancy might have been caused by differences in the mouse haplotype or the sources of TT and CT. Despite the discrepancy, our current findings emphasize the effectiveness of the newly established NKM 16–2-4 for the targeting of vaccine antigen to M cells to induce antigen-specific immune responses.

Moreover, when mice were orally immunized with botulinum toxoid (BT) conjugated with NKM 16–2-4 or control rat IgG (in total, each 200 μg contained 50 μg BT per mouse) in the presence of CT, brisk botulinum toxin–specific serum IgG and fecal IgA responses were induced in mice immunized with BT-conjugated NKM 16–2-4, but not in those immunized with BT-conjugated control rat IgG (Fig. 2 C). In addition, the mice immunized with BT-conjugated NKM 16–2-4 survived after challenge with 200 ng (10,000× LD_{50}) of botulinum toxin, whereas the mice immunized with BT-conjugated control rat IgG died within 3 h (Fig. 2 D). These data strongly indicate that the M cell-targeted mucosal vaccine with NKM 16–2-4 can effectively induce protective immunity with the minimum dose of vaccine antigen.

To confirm the mechanism by which the NKM 16–2-4–based M cell–targeted mucosal vaccine induces brisk antigen-specific immune responses in the systemic and mucosal compartments, and its universality, OVA was then chosen as a prototype antigen with low antigenicity. An immunocytochemical analysis revealed that Alexa Fluor 647–labeled OVA conjugated with NKM 16–2-4 and FITC-conjugated avidin specifically reacted with UEA-1–positive isolated M cells in vitro (Fig. 3 A), and intestinal loop assay clearly demonstrated that it specifically attached to the apical surfaces of M cells and was subsequently taken up into the cytoplasmic regions of M cells in vivo (Fig. 3 B). Furthermore, brisk increases in the levels of OVA-specific serum IgG were induced in mice immunized with only 200 μg OVA-conjugated NKM 16–2-4 (containing 50 μg OVA), but not with the same amount of OVA-conjugated control rat IgG (Fig. 3 C). Our previous study showed that amounts of OVA as high as 1 mg were required to induce OVA-specific immune responses (5); now, oral immunization with even small amounts of poorly immunogenic antigens (e.g., OVA) is possible by using the M cell–targeting concept with NKM 16–2-4.

We could not directly compare the efficacy of NKM 16–2-4–based mucosal vaccine with those of already published σ1-based mucosal vaccines (10, 11) because the latter systems have been used for nasal, but not oral, vaccines and no information is currently available on whether σ1 possesses

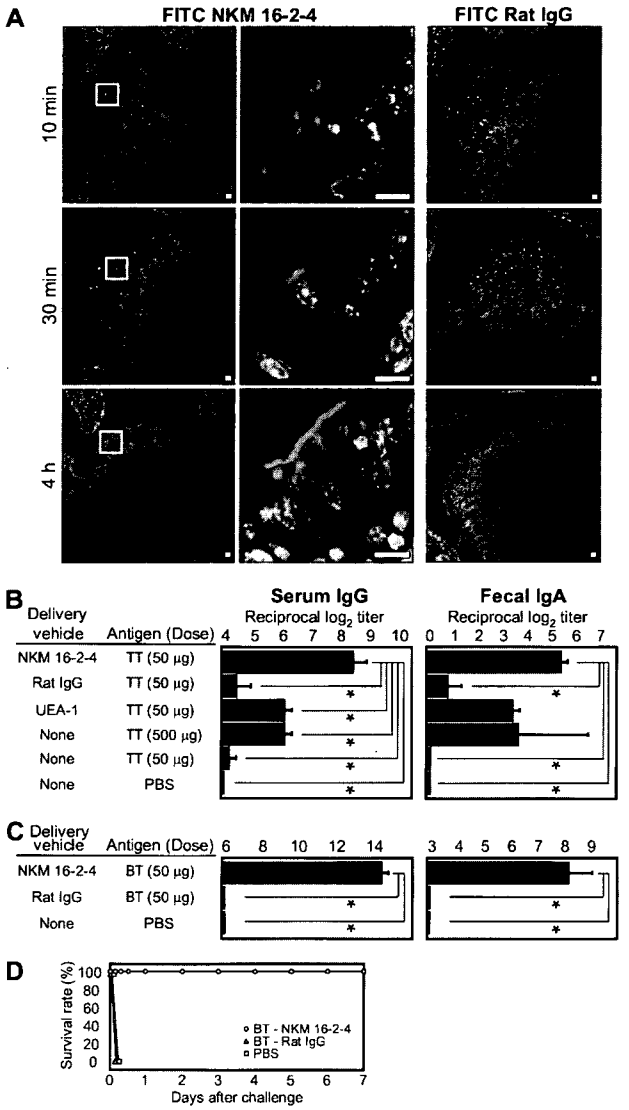

Figure 2. Development of an M cell–targeted mucosal vaccine with NKM 16–2-4. (A) FITC-conjugated NKM 16–2-4, but not FITC-conjugated control rat IgG, was specifically attached to the apical surfaces of M cells in FAE of PPs within 10 min of inoculation in an intestinal loop assay. The NKM 16–2-4 was subsequently taken up into the cytoplasmic regions of M cells within 30 min and reached the basal membrane of M cells within 4 h. Bars, 10 μm. (B) TT conjugated with NKM 16–2-4 effectively induced high-level, TT-specific serum IgG and fecal IgA responses, unlike TT conjugated with control rat IgG or UEA-1. Furthermore, the levels were superior to those in mice immunized with 10 times the amount of noncoupled TT (500 μg). *, $P < 0.01$, Tukey's t test. (C) BT-conjugated NKM 16–2-4, but not BT-conjugated control rat IgG, induced brisk botulinum toxin–specific serum IgG and fecal IgA responses. (D) Mice orally immunized with BT-conjugated NKM 16–2-4 were protected from an i.p. challenge with 10,000× LD_{50} type A botulinum toxin. Data are expressed as the mean ± the SD.

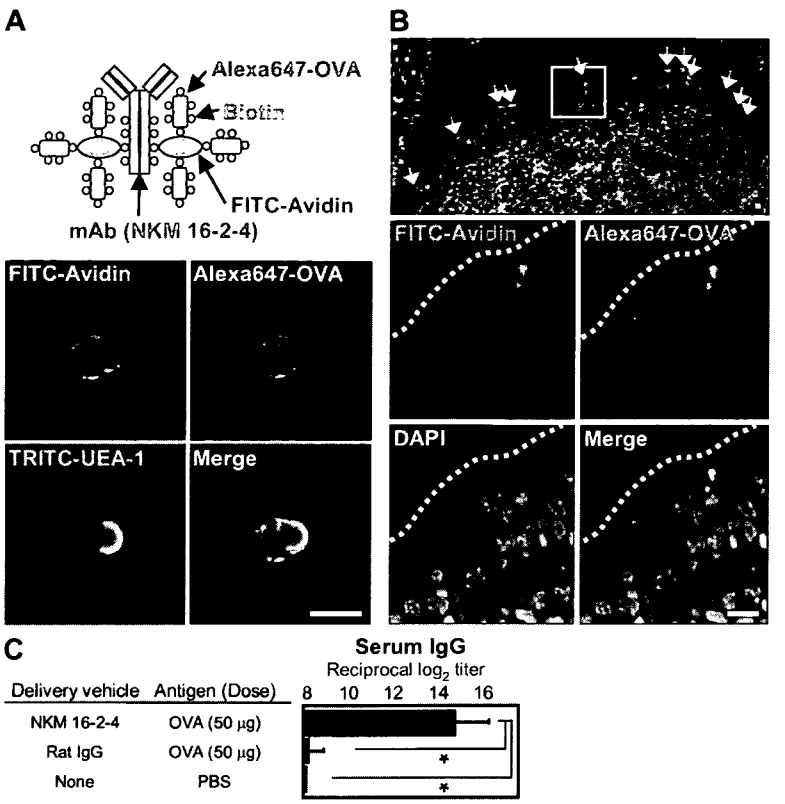

Figure 3. Effective uptake and universality of the M cell–targeted mucosal vaccine. (A) Immunocytochemical analysis showed that an M cell–targeted OVA vaccine composed of Alexa Fluor 647–conjugated OVA, FITC-conjugated avidin, and NKM 16-2-4 specifically reacted with isolated UEA-1–positive M cells. (B) In an intestinal loop assay, the M cell–targeted OVA specifically attached to the apical surfaces of M cells (red arrows) and was immediately taken up into the cytoplasmic regions of M cells. Bars, 10 μm. (C) Orally administered OVA-conjugated NKM 16-2-4 effectively induced an OVA-specific serum IgG response, whereas an OVA-conjugated control rat IgG did not. Data are expressed as the mean ± the SD.

specificity for villous M cells. However, our strategy for using NKM 16–2-4 as an M cell–targeting vehicle might be superior, because NKM 16–2-4 possesses specificity for both villous M cells and PP-associated M cells. In support of our hypothesis, our previous data showed that villous M cells are capable of taking up orally administered antigens for the induction of PP-independent, antigen-specific immune responses (4). However, it should be noted that TT- or OVA-specific immune responses were not effectively induced without the presence of the mucosal adjuvant CT, even if the antigen was targeted to M cells by using NKM 16–2-4. This finding could be explained by the observation that the gastrointestinal immune system generally operates via a sophisticated mucosal regulatory network to avoid unnecessary hyperimmune responses to the numerous orally encountered antigens in the harsh environment of the intestinal tract (3). Therefore, it is essential to use the mucosal adjuvant, which temporarily breaks the mucosal regulatory network system, to activate gastrointestinal immunity. In practical terms, further studies are needed to develop a safe mucosal adjuvant and take advantage of M cell–targeted mucosal vaccines with NKM 16–2-4.

Identification of antigens recognized by NKM 16–2-4

In attempts to elucidate the antigen-sampling mechanism of M cells for the induction of antigen-specific immune responses, a major drawback has been the lack of knowledge of the specific genes and the corresponding molecules expressed by M cells. In addition, no information regarding which murine M cell–specific glycoproteins are recognized by UEA-1 is currently available, although UEA-1 is used extensively as a specific marker of M cells in mice. Therefore, we tried to identify the membrane antigen recognized by NKM 16–2-4 by using a proteomics approach with liquid chromatography–tandem mass spectrometry (LC-MS/MS) after immunoprecipitation of an M cell lysate with NKM 16–2-4. 4 major bands (3 bands >250 kD and 1 band of ~150 kD) were precipitated by NKM 16–2-4 (Fig. 4 A), and these were identified by LC-MS/MS as maltase glucoamylase (top three bands) and alanyl (membrane) aminopeptidase (bottom band). These two molecules, which have been reported as intestinal enzymes of 410, 275, and 260 kD (21), and 150 kD, respectively, (22) under denatured conditions, are distributed at the brush borders of epithelial cells for the final digestion of dietary nutrients (21, 22). Because they were not homologous